



## Review Article

## Recent advances in multidimensional (1D, 2D, and 3D) Joule heating devices based on cellulose: Design, structure, application, and perspective



Chuanyin Xiong<sup>a,1,\*</sup>, Mengjie Zhao<sup>a,1</sup>, Tianxu Wang<sup>a,1,\*</sup>, Jing Han<sup>b</sup>, Yongkang Zhang<sup>a</sup>, Zhao Zhang<sup>a,\*</sup>, Xianglin Ji<sup>c,\*</sup>, Qing Xiong<sup>a</sup>, Yonghao Ni<sup>d,e</sup>

<sup>a</sup> College of Bioresources Chemical & Materials Engineering, Shaanxi University of Science and Technology, Xi'an 710021, China

<sup>b</sup> School of Materials Science and Engineering, Tianjin Polytechnic University, Tianjin 300387, China

<sup>c</sup> Oxford-CityU Centre for Cerebro-Cardiovascular Health Engineering (COCHE), City University of Hong Kong, Hong Kong SAR, 999077, China

<sup>d</sup> Department of Chemical and biomedical Engineering, The University of Maine, Orono, Maine, 04469, USA

<sup>e</sup> University of New Brunswick, Limerick Pulp & Paper Ctr, Fredericton, NB E3B 5A3, Canada

## ARTICLE INFO

## Article history:

Received 22 December 2023

Revised 24 March 2024

Accepted 8 April 2024

Available online 24 April 2024

## Keywords:

Cellulose

Multidimensional

Joule heating

Design

Preparation

## ABSTRACT

The demand for flexible electric heating devices has increased due to technology advancement and improved living standards. These devices have various applications including personal thermal management, hyperthermia, defrosting, agricultural heating film, and oil-water separation. Joule heat, generated by electric currents, is commonly used in electrical appliances. To incorporate Joule heating into flexible electronics, new materials with excellent mechanical properties are necessary. Traditional polymers, used as reinforcements, limit the continuity of conductive networks in composites. Therefore, there is a need to develop flexible Joule thermal composite materials with enhanced mechanical strength and conductivity. Cellulose, a widely available renewable resource, is attracting attention for its excellent mechanical properties. It can be used as a dispersant and reinforcing agent for conductive fillers in cellulose-based composites, creating highly conductive networks. Various forms of cellulose, such as wood, nanocellulose, pulp fiber, bacterial cellulose, cellulose paper, textile clothing, and aramid fiber, have been utilized to achieve high-performance Joule thermal composites. Researchers have achieved excellent mechanical properties and developed efficient electric heating devices by designing cellulose-based composites with different structures. The scalable production methods enable large-scale application of cellulose-based devices, each with unique advantages in 1D, 2D, and 3D structures. This review summarizes recent advancements in cellulose-based Joule thermal composites, providing insights into different structural devices, and discussing prospects and challenges in the field.

© 2025 Published by Elsevier Ltd on behalf of The editorial office of Journal of Materials Science & Technology.

## 1. Introduction

With the rapid development of technology and the continuous improvement of people's living standards, flexible electric heating devices have received widespread attention [1–5]. And it has been applied to our daily life and various fields of industrial production, such as personal thermal management [6], hyperthermia [7], defrosting [8], agricultural heating film [9], and oil-water separation [10]. The heat generated when an electric current passes through

a conductor is called Joule heat [11]. This type of heat energy is very common in our daily lives, such as incandescent lamps, electric furnace wires, and electric water heaters. With the continuous improvement of people's cognitive level, Joule heating is also used in the field of flexible electronics, namely flexible Joule heating devices [12–15]. A Joule thermal device is a functional device that converts the voltage of an external load into heat. This device has a high requirement for the internal conductivity of the material, and the conductive network inside the material directly determines the performance parameters of electric heating. At present, conductive materials used for electric heating devices include carbon materials [16], metals [17], and conductive polymers [18]. However, it is difficult to achieve practical mechanical performance by directly using conductive materials in flexible Joule thermal devices. This requires

\* Corresponding authors.

E-mail addresses: [xiongchuanyin@126.com](mailto:xiongchuanyin@126.com) (C. Xiong), [2425176812@qq.com](mailto:2425176812@qq.com) (T. Wang), [zhangzhaogq@sust.edu.cn](mailto:zhangzhaogq@sust.edu.cn) (Z. Zhang), [xianglij3-c@my.cityu.edu.hk](mailto:xianglij3-c@my.cityu.edu.hk) (X. Ji).

<sup>1</sup> These authors contributed equally to this work.

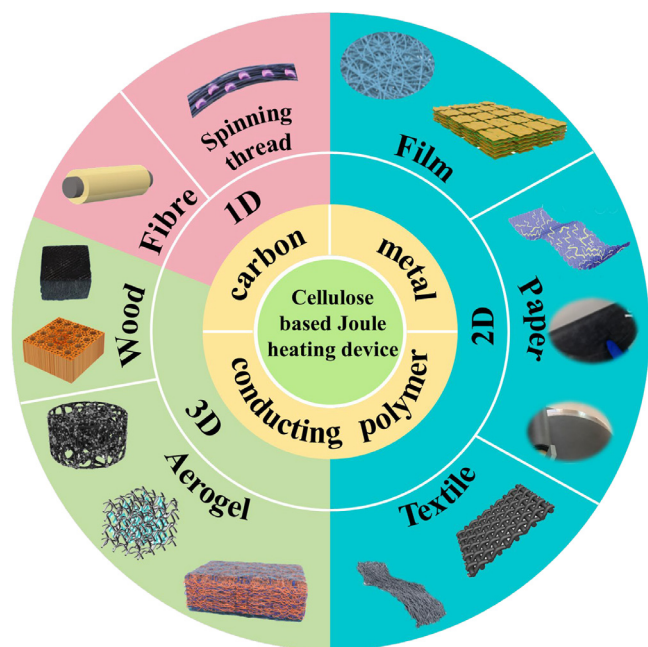


**Fig. 1.** Cellulose-based Joule thermal devices with different structures (1D, 2D, and 3D). Fibre [64]. Spinning thread [57]. Film [91,101]. Paper [88,89,100]. Textile [90,97]. Aerogel [132,133]. Wood [124,127].

a matrix material with excellent mechanical properties to enhance its mechanical properties. The mechanical reinforcements used in traditional flexible electronic devices are polymers (plastics, resins, rubber, etc.) [19–21]. Although these reinforcements can endow flexible Joule thermal composites with excellent mechanical properties, they also have many fatal drawbacks. For example, it is difficult to ensure the continuity of the conductive network inside the composite material obtained by combining these polymer materials with conductive active substances. This is very detrimental to the practical application of flexible Joule thermal devices. Therefore, it is necessary to develop flexible Joule thermal composite materials with high strength and high conductivity networks.

Cellulose is a widely sourced and renewable biomass resource [22]. Due to its excellent aspect ratio and mechanical properties, it has been widely used in fields such as energy storage [23], sensing [24], electromagnetic shielding [25], and electric heating [26]. More importantly, within cellulose-based Joule thermal composites, due to their large aspect ratio, cellulose can serve as a dispersant and reinforcing agent for conductive fillers [27]. And it has played a very positive role in the construction of high-conductivity networks. This is beneficial for the preparation of high-strength and high-conductivity Joule thermal devices. In recent years, cellulose, including wood [28], nanocellulose [29], pulp fiber [30], bacterial cellulose [31], cellulose paper [32], textile clothing [33], and aramid fiber [34], has been used to prepare high-performance cellulose based Joule thermal composites. In recent research work, through the design of cellulose-based Joule thermal composites with different structures, including one-dimensional structures (1D fiber and spinning thread), two-dimensional structures (2D film, paper, and textile clothing), and three-dimensional structures (3D wood and aerogel), excellent mechanical properties and the vigorous development of electric heating performance devices have been achieved (Fig. 1). More importantly, cellulose-based devices can be manufactured on a scale using cost-effective methods such as papermaking [35], printing [36], and spraying [37] to achieve commercial large-scale applications. In addition, with the deepening of research on cellulose-based Joule thermal devices, more attention should be paid to the practicality and stability of the de-

vices themselves. Devices with different structures have unique advantages. For example, 1D cellulose devices have a large aspect ratio, 2D devices can achieve integration of electromagnetic shielding, sensing, and electric heating devices, while 3D structure devices have a larger heating area. Therefore, it is necessary to summarize the research work on cellulose-based Joule thermal devices with different structures (1D, 2D, and 3D). This article reviews the latest research progress in 1D, 2D, and 3D Joule thermal composites based on cellulose from the perspective of devices with different structures in recent years. Finally, we shared some prospects and challenges in the field of cellulose-based Joule thermal devices.

## 2. Structural design and application of (1D, 2D, and 3D) cellulose-based Joule heating composite materials

The design of cellulose-based Joule thermal composites with different structures mainly relies on various preparation processes. Fig. 2 shows the main preparation methods of Joule thermal devices based on different structures of cellulose. The 1D structure is mainly achieved through impregnation [38], wet spinning [39], and in-situ growth [40]. The 2D structure is mainly prepared through methods such as deposition [41], vacuum filtration [42], paper-making [43], and controllable sputtering [44]. The 3D structure is mainly to construct conductive gel through freeze drying [45]. In addition, in-situ growth and the use of natural wood's porous structure can also achieve the construction of 3D structures [46,47].

### 2.1. 1D cellulose-based composite materials designed for Joule heating

The flexible Joule heating device based on 1D cellulose has the advantages of small size, lightweight, and portability, which has attracted extensive attention from scientists in the field of wearable personal thermal management. More importantly, thanks to its excellent aspect ratio, 1D fibers are easily sewn onto clothing for use in the human body's thermal management system. Due to cellulose being an excellent renewable biomass resource, carbonization can enhance its conductivity to prepare cellulose carbon-based materials with Joule thermal properties. In addition, cellulose-based Joule thermal composites with excellent performance can also be obtained by compounding cellulose with other conductive components through preparation processes such as wet spinning and immersion coating. And these two processes can achieve large-scale preparation, so Joule thermal composite materials based on 1D cellulose show great application prospects in wearable devices.

#### 2.1.1. 1D cellulose carbon-based composite materials

Due to the lack of conductivity of cellulose itself, carbonization has become the simplest method to make it conductive [48]. However, the mechanical properties of carbonized cellulose carbon-based strength of materials are poor. Based on this, Li et al. [49] combined cotton fibers with ceramics and prepared cellulose-based electrically heated carbon-based material using the carbonization method. Fig. 3(A) shows the preparation process of cellulose/ceramic electrothermal materials. Firstly, twist the cellulose fabric into a thick thread to obtain 1D cellulose carbon precursor material. Then place it in an oven for pre-oxidation. Finally, the 1D cellulose carbon-based electric heating material is obtained by high-pressure molding with ceramics and carbonization. In this work, the author discussed the effect of the number of cellulose yarns on the Joule thermal properties. As shown in Fig. 3(B), with the increase of yarn count, the cellulose carbon-based material (C64) of 64 cellulose yarns exhibits the most excellent electric heating performance (120.4 °C) at the same voltage (8 V). And the composite material C64 exhibits excellent thermal stability performance. As the heating time increases, the thermal energy emitted



**Fig. 2.** Main preparation methods for 1D, 2D, and 3D cellulose-based Joule thermal devices. Immersion [56]. Wet spinning [57]. In-situ [68]. Deposition [97]. Vacuum filtration [101]. Paper-making [88]. Freeze-drying [133]. Wood [124].

by C64 is evenly distributed around the 1D cellulose carbon-based material. This is due to the excellent thermal conductivity of the surrounding ceramic materials. The ceramic materials used in this work effectively and uniformly disperse the heat energy emitted by 1D cellulose carbon materials, making them of great application value in indoor temperature control. However, direct carbonization severely damages the mechanical properties of cellulose itself. Composite with highly conductive active substances such as carbon materials [50], metals [51], and conductive polymers [52] has become an ideal method for preparing cellulose-based Joule thermal devices with excellent mechanical properties.

### 2.1.2. 1D cellulose/carbon (GR, CNT) composite materials

In the preparation of existing 1D cellulose/carbon Joule thermal composite materials. Graphene and carbon nanotubes have been widely used in the field of electric heating devices because of their special micro morphology, excellent electrical conductivity, and good processability [53,54]. Cellulose-based yarns have excellent mechanical properties and have a large number of hydroxyl tube energy groups on their surface [55]. It can provide a large number of active sites for the adsorption of Graphene. Wu et al. [56] prepared an electrically heated yarn of 1D cellulose cotton fiber coated with Graphene by ultrasonic impregnation (Fig. 3(C)). On the one hand, the composite material has excellent mechanical properties of cotton yarn. On the other hand, the continuous loading of Graphene on the surface of cellulose fabric also provides it with excellent electrical conductivity. At the same time, it also ex-

hibits excellent electrical heating performance. Different 1D cotton fiber/Graphene composites were obtained by controlling the yarn diameter. As shown in Fig. 3(D), the composite material with a diameter of 3.5 mm has an electrical heating performance of 70 °C at a safe voltage of 20 V. And the stability of the composite material is enhanced through the coating protection of PDMS. In addition, two 1D cotton fiber/Graphene composites with different diameters still maintain good electric heating performance after cleaning. The cellulose-based cotton fabric/Graphene composite prepared in this work has promoted large-scale preparation and development in the field of personal fabric thermal management.

However, the impregnation process can only prepare a core-shell structure based on cellulose and electrically heated active substances, with cellulose as the core, and the active substances form a continuous conductive shell structure on the surface of the cellulose material through electrostatic adsorption. During use, the continuous bending of this structure will inevitably cause the detachment of electrically active substances, thereby seriously affecting the electrical heating performance of the device. Therefore, the 1D composite material prepared by uniformly mixing cellulose and active substances through wet spinning can fully solve this problem. On the one hand, cellulose can provide excellent mechanical properties and can tightly lock conductive substances in composite materials through sufficient dispersion and winding. On the other hand, conductive active substances (such as CNTs) can form good conductive pathways within the composite material to provide electrical heating performance. Jing et al. [57] pre-



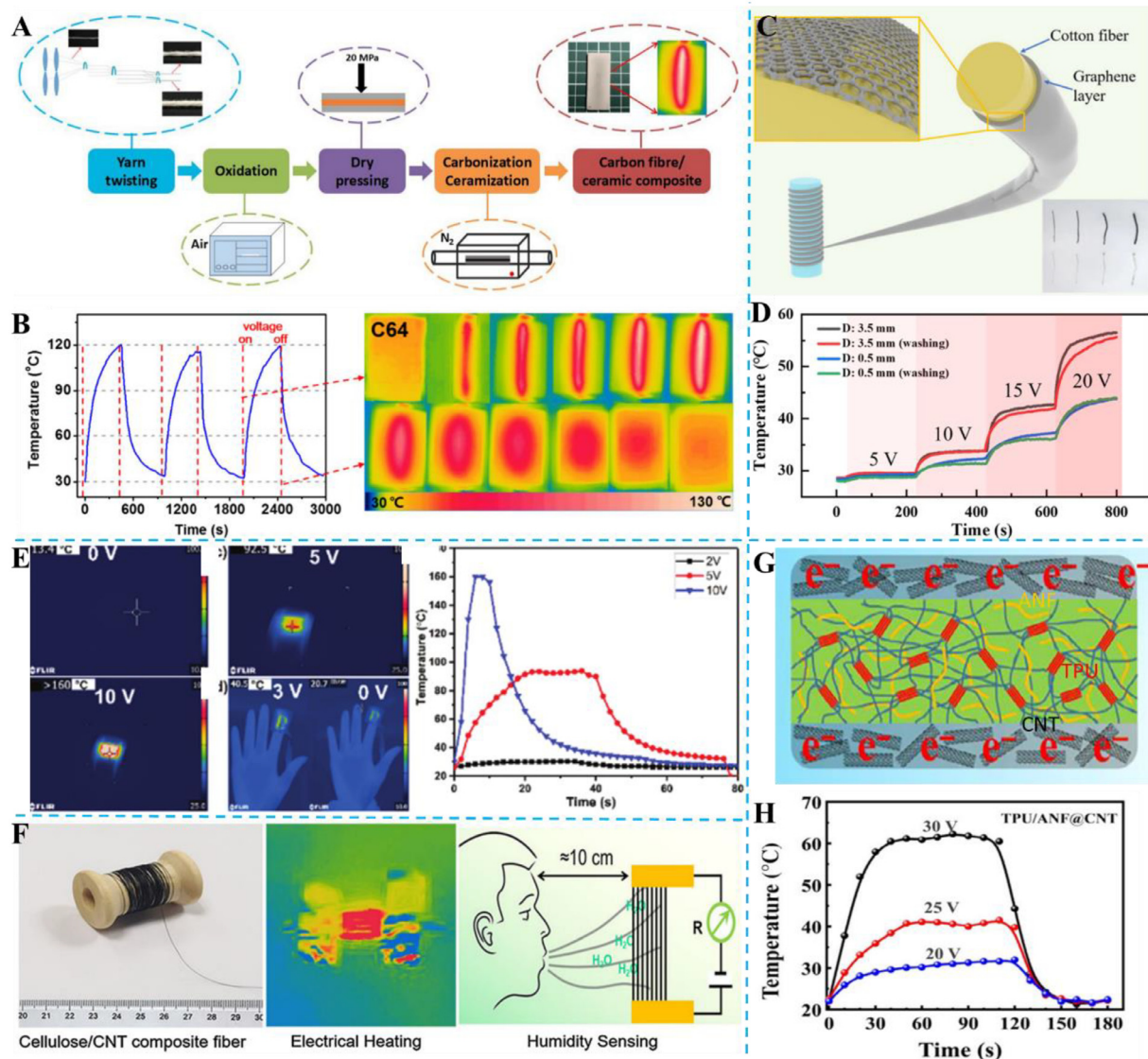


**Fig. 3.** (A) The preparation process of 1D cotton fiber/ceramic electric heating material. (B) The electrothermal performance of 1D cotton fiber/ceramic under an applied voltage of 8 V [49]. (C) Schematic diagram of 1D cellulose cotton fiber yarn coated with Graphene. The illustrations are physical images. (D) Changes in the electrothermal properties of composite materials after washing for 2 h under different applied voltages [56]. (E) Under different applied voltages CNTs@Cellulose Evolution of heating temperature for composite fibers [57]. (F) Physical diagram of C/CNT composite fiber, schematic diagram of Joule heat and humidity sensing [58]. (G) TPU/ANF@CNT structural schematic diagram of composite materials. (H) Time and temperature variation curves of TPU/ANF@CNT composite fibers under different voltages [61].

pared a cellulose/CNT composite material by mixing cellulose and CNT in a certain proportion and using a wet spinning process (CNTs@Cellulose). Thanks to the barrier effect between cellulose and CNT, within the composite material, these two act as barriers to prevent the aggregation of each other. Among them, cellulose provides excellent mechanical properties, and due to its barrier effect internally, CNT forms a uniformly dispersed conductive pathway ( $871.55 \text{ S m}^{-1}$ ). As shown in Fig. 3(E), CNTs@Cellulose shows excellent electrical heating performance. At a voltage of 10 V, the composite material exhibits a heating performance of 160 °C. In addition, due to CNTs@Cellulose, the composite material exhibits excellent flexibility and conductivity, as well as excellent sensing performance. It can monitor the real-time movement of human joint parts in real-time. And the author also achieved this through this process CNTs@Cellulose large scale preparation. The results indicate that the composite material exhibits excellent application functions in both electric heating and sensing. It has certain appli-

cation value in the field of multifunctional intelligent textile fiber products for human thermal management and sensing detection in the future. Similarly, as shown in Fig. 3(F), Ma et al. [58] prepared carboxylated CNT/cellulose composite materials (C/CNT) for electric heating and humidity sensing through a wet spinning process. The results show that the C/CNT-20 composite material obtained when the CNT content is 20 % has the best mechanical properties ( $185 \pm 9 \text{ MPa}$ ) and electrical heating performance. Under an applied voltage of 9 V, C/CNT-20 can reach a temperature exceeding 55 °C in 15 s. In addition, due to the swelling effect of cellulose in contact with water molecules, the resistance of the composite material changes, and C/CNT-20 also exhibits certain humidity sensing performance. This fiber can be used for intelligent flexible fabric design and wearable devices. Aramid nanofiber (ANF) is a high-performance fiber material with excellent mechanical properties and a high aspect ratio [59,60]. This material also exhibits excellent dispersion and enhancement effects on nanoelectric heat-



ing active substances. For example, He et al. [61] used wet spinning and a two-step drying process to prepare ANF/Thermoplastic polyurethane (TPU)/CNT composites (TPU/ANF@CNT). Firstly, TPU and ANF were wet spun to obtain 1D fibrous composite materials. Then, after drying, a TPU/ANF@CNT composite material with a core-shell structure was obtained by immersion in the TPU/CNT composite slurry (Fig. 3(G)). In this material, the internal “core” structure TPU/ANF provides excellent mechanical support performance. The external “shell” structure TPU/CNT provides sufficient conductivity for the composite material. Due to the use of TPU as the supporting material in the external shell structure, this will have a certain impact on the construction of conductive structures. The results show that the composite material exhibits electrical heating performance between 30 and 62 °C at a voltage of 20–30 V (Fig. 3(H)). This performance is slightly inferior to the performance of previous works. However, using TPU as the protective structure of conductive material CNT also prevents the detachment of electrically active substances during use. Therefore, in the preparation of 1D cellulose CNT composite electrothermal materials, the best choice is to directly configure cellulose and CNT as a slurry, and then obtain the composite material through a certain preparation process.

### 2.1.3. 1D cellulose/metal composite materials

Compared to carbon materials, metal materials have more free electrons, so their conductivity is relatively high [62]. In addition, metal materials also have certain antibacterial properties. It can effectively protect human health and safety while being used as a thermal management device for the human body. Hu et al. [63] prepared a conductive cellulose cotton yarn with dual functions of sensing and Joule heating. Fig. 4(A) shows the preparation process of conductive yarn. Firstly, silver ions are adsorbed on the surface of cotton yarn through adsorption. Then, a conductive yarn based on metallic silver is obtained through a reduction reaction. In order to enhance its conductivity, an MXene@Ag@CY composite material was obtained by coating a layer of MXene conductive layer on its surface through a simple impregnation process. Thanks to the high conductivity of metallic silver and MXene ( $22 \Omega \text{ cm}^{-1}$ ), the temperature of MXene@Ag@CY composite material reached 92 °C under a constant external load voltage of 6 V. It is worth mentioning that MXene@Ag@CY also exhibits excellent tensile properties. When the tensile strain increases from the initial state to 11 %, it still exhibits stable electrical heating performance. The excellent mechanical properties also endow the composite material with certain sensing properties. The author achieved over 55 % strain on clothing by weaving 1D conductive cellulose yarn in a certain way. This is far superior to the strain sensors currently reported. In summary, this conductive yarn has certain application prospects in the fields of motion detection, health tracking, and electrothermal medicine. MXene-based conductive fiber materials prepared by the impregnation process still have the problem of easy detachment, which seriously affects the service life of electric heating materials. In addition, in large-scale preparation processes, the impregnation process is difficult to ensure consistency in the concentration of the active substance slurry. It is difficult to control the uniform distribution of active substances in the large-scale preparation of devices. Based on this, in order to solve this problem, Wang et al. [64] prepared a 1D aramid fiber-based electric heating composite material with a conductive core (MXene) shell (ANF) structure. Fig. 4(B) shows the preparation process of MXene@ANF composite material. From the figure, it can be seen that the structure is controlled by a dual-in and single-out mold. Firstly, place the prepared ANF solution and MXene solution in a wet spinning syringe. Then control the synchronous extrusion of the two syringes. Finally, by combining the two materials in the mold, a 1D composite material with MXene as the core and ANF as

the shell can be obtained. The microstructure of the composite material can be clearly observed through SEM images (Fig. 4(C)). On the one hand, the internal MXene exhibits a continuous and dense structure, providing excellent conductivity ( $2515 \text{ S m}^{-1}$ ) (Fig. 4(D)). On the other hand, due to self-assembly, the external ANF exhibits ordered nanofiber-like morphology, providing excellent mechanical properties (tensile strength up to 130 MPa) for composite materials. Therefore, under the synergistic effect of ANF and MXene, the composite material exhibits excellent electrical heating performance and flexibility. Under an applied voltage of 3–21 V, the MXene@ANF composite material exhibits electrothermal properties at 25–123 °C (Fig. 4(E, F)). Thanks to the high conductivity of MXene, the composite material also exhibits sensitive detection of multiple bending deformations (response time of 100 ms, recovery time of 98 ms). Therefore, MXene@ANF composite materials with enhanced mechanical structural properties have shown great potential in electric heating and intelligent sensing wearable devices. And the 1D structure proposed in this work to protect conductive active substances is a method worth further development and application.

### 2.1.4. 1D cellulose/conductive polymer composite materials

Conductive polymers (such as Polypyrrole (PPy) and poly (3,4-ethylenedioxythiophene): poly (4-styrenesulfonate) (PEDOT: PSS)) have been used in the field of electric heating due to their excellent conductivity [65,66]. As shown in Fig. 5(A), Lv et al. [67] obtained Polypyrrole coated cellulose composite yarn material (PCLY) by loading PPy on the surface of commercial regenerated cellulose yarn through in-situ polymerization. Thanks to the conductivity and energy storage performance of Polypyrrole, PCLY has two application functions: electric heating and electrochemical energy storage. Under an applied voltage of 6 V, the 1D-PCLY composite material exhibited a heating temperature of 106.6 °C. And the electrically heated fabric made of PCLY composite material still maintains stable electrical heating performance after being placed for a long time and washed multiple times, indicating its ultra-high stability in use. In addition, flexible energy storage devices woven with PCLY also exhibit good performance ( $663 \text{ mF cm}^{-2}$  at  $1 \text{ mA cm}^{-2}$ ). PEDOT: PSS is also used in the preparation of electric heating devices due to its high thermal and mechanical stability. As shown in Fig. 5(B), Pattanarat et al. [68] prepared PEDOT: PSS@cotton yarn cellulose-based composites for Joule heating. Firstly, the bare cotton yarn is polymerized in situ to load PEDOT: PSS onto its surface. Then, the phase separation of PEDOT and PSS was achieved through ethylene glycol (EG) to obtain 1D-EG/PEDOT: PSS composite material with high conductivity ( $76 \text{ S cm}^{-1}$ ). The conductivity diagram of 1D-EG/PEDOT: PSS yarn is shown in Fig. 5(C). The results indicate that the resistance value of the composite material treated with EG is much lower than that of the untreated yarn. This is because EG covers the external area of PEDOT, achieving a good barrier effect between PEDOT and PSS. Thanks to the high conductivity structure after EG treatment, the 1D-EG/PEDOT: PSS composite material can reach an electric heating temperature of 150 °C in a short time (10 s) under an applied voltage of 5 V (Fig. 5(D)). In addition, after bending the conductive yarn at 50°, there was no significant change in its electric heating performance. And after 2000 stretching release cycles, the resistance of the conductive yarn only increased by 1.19 times compared to the original state, demonstrating excellent durability and stability.

Based on the above summary of 1D cellulose-based Joule thermal composite materials. Structural design is crucial for the mechanical and electrical heating properties of 1D cellulose-based Joule thermal composites. At present, impregnation and in-situ polymerization are the main methods for preparing composite electric heating materials based on fabrics. The impregnation pro-

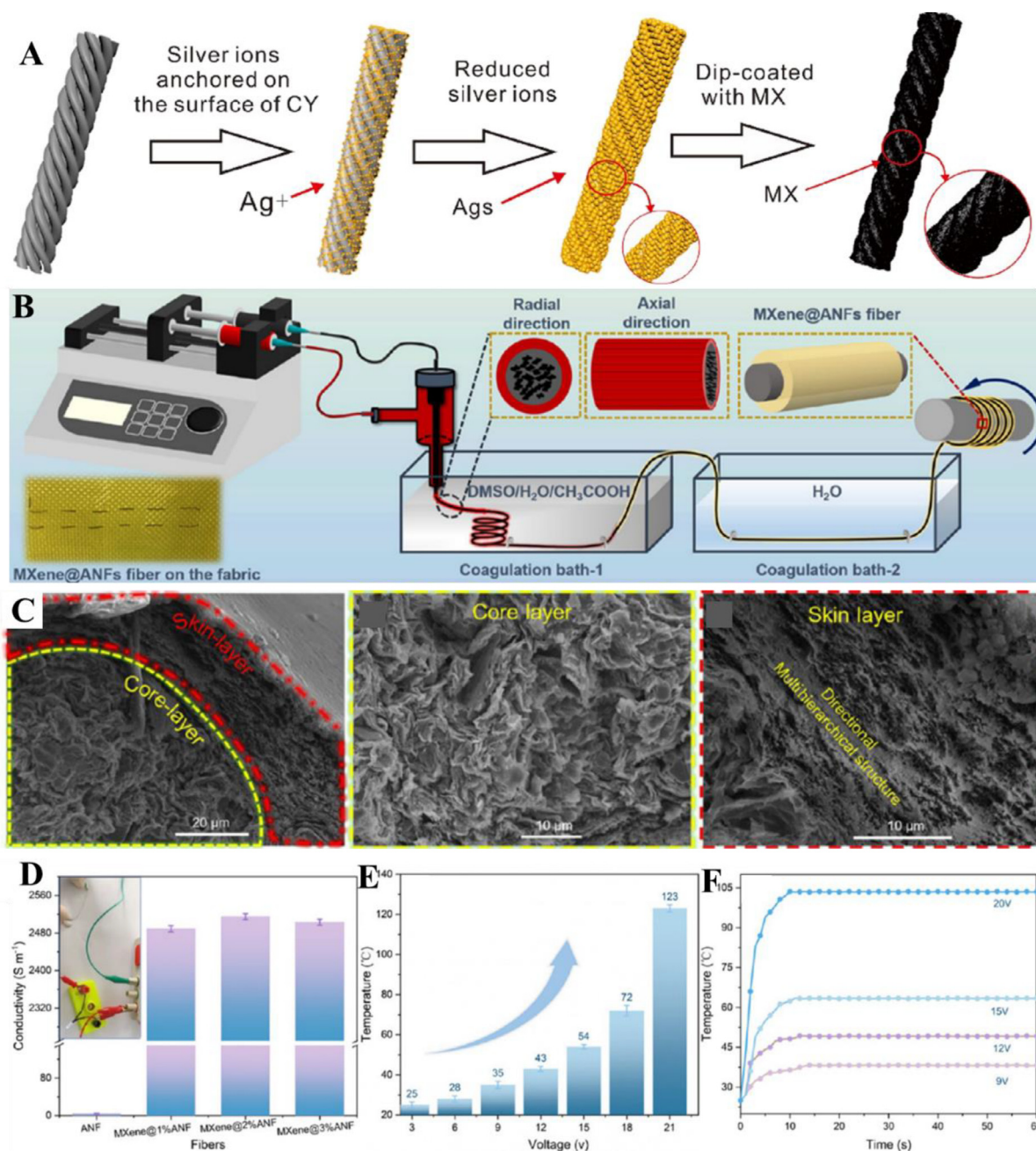


**Fig. 4.** (A) Preparation process of MXene@Ag@CY composite material [63]. (B) The preparation process of MXene@ANF composite materials. (C) The microstructure of MXene@ANF composite material. (D) The conductivity of MXene@ANF. (E) The electric heating temperature of MXene@ANF under different voltages. (F) The relationship between the time and temperature changes of MXene@ANF under different voltages [64].

process can ensure the service life of the device, and adding an adhesive to the impregnation process can also have a certain impact on its conductivity. Therefore, in-situ polymerization is a relatively suitable preparation method. In addition, for smaller-sized cellulose materials (such as nanocellulose, aramid fibers, etc.), wet spinning is the most important preparation method. Structural design still plays a crucial role in the performance of devices. As mentioned earlier, in core-shell structures, blending cellulose with active substances or constructing composite materials with active substances as shell structures is the best structure for improving service life and electrothermal performance. In terms of application, 1D cellulose-based electric heating composite materials are mainly used in the fields of thermal therapy and flexible wearable intelligent fabric thermal management. For example, during the

Winter Olympics, in order to ensure the best athletic performance of athletes, Chinese researchers provided a graphene-based smart fabric, including seats, carpets, tables, and various wearable fabrics. It can ensure that the physical functions of staff and athletes remain stable in cold conditions. Table 1 compares the main performance parameters of different 1D cellulose-based electric heating composites.

## 2.2. 2D cellulose-based composite materials designed for Joule heating

2D cellulose-based Joule thermal composite materials are more inclined towards paper [69], film [70], and textile clothing [71], which have a larger heating area and heat transfer surface. From

**Table 1**  
Performance parameters of 1D cellulose Joule thermal composite material.

Material	Voltage (V)	Temperature (°C)	Response time (s)	Recovery time (s)	Refs.
C64	10	188.7	400	–	[49]
cotton fiber/Graphene	20	70	50	–	[56]
CNTs@Cellulose	10	160	8	50	[57]
C/CNT	9	55	15	25	[58]
TPU/ANF@CNT	30	62	40	40	[61]
MXene@Ag@CY	6	92	5	8	[63]
MXene@ANF	21	123	10	–	[64]
PCLY	6	106.6	220	130	[67]
EG/PEDOT:PSS	5	150	10	10	[68]

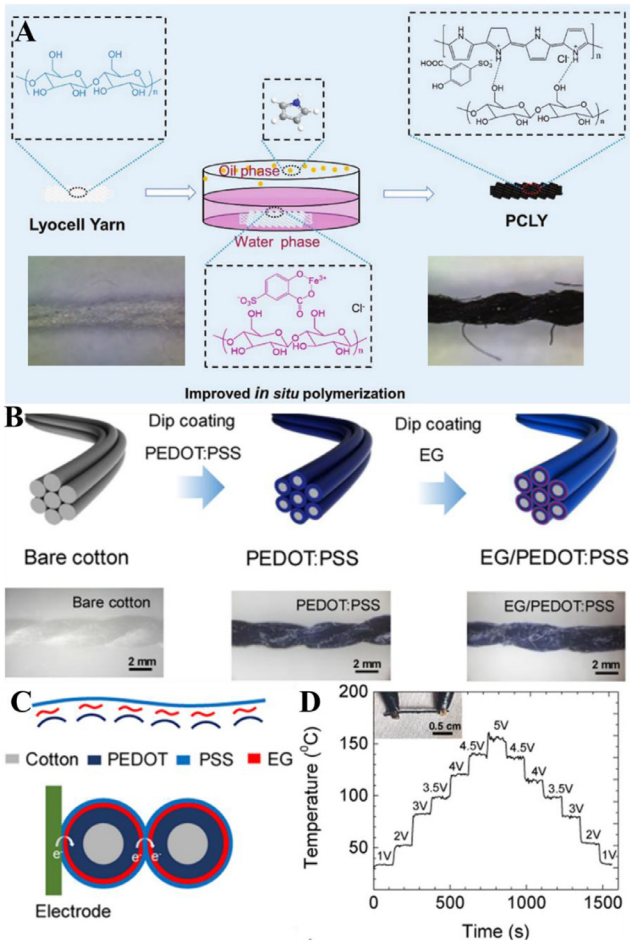


**Fig. 5.** (A) Preparation process of PCLY composite material. The illustrations are physical images of the materials [67]. (B) The preparation process of 1D-EG/PEDOT:PSS composite material. (C) 1D-EG/PEDOT: Conductivity diagram of PSS composite material. (D) Temperature and time evolution of 1D-EG/PEDOT: PSS composite materials under different voltages [68].

a practical application perspective, cellulose-based paper and film are the most common 2D Joule thermal devices. Among them, paper based on papermaking technology can achieve large-scale manufacturing. And it can be cut into various shapes to meet the demand for Joule thermal devices in people's daily lives. Unlike 1D cellulose-based Joule heating devices, 2D electric heating devices can generate a larger heating area. When used in human thermal management systems, it can have better contact with the human body and generate stable thermal signals. In general, 2D cellulose-based Joule thermal devices are designed and prepared by using cellulose and electroactive substances (such as Graphene [72], car-

bon nanotubes [73,74], and MXene [75]) through vacuum filtration, spraying, coating, and other preparation processes. In addition, introducing metal materials and conductive polymers into the surface of cellulose paper or textile fabrics through in-situ growth is also the main method for preparing 2D cellulose Joule thermal devices.

2.2.1. 2D cellulose/carbon composite materials

Carbon materials include conductive carbon black, activated carbon, Graphene, and carbon nanotubes. In the application of Joule thermal devices, a continuous conductive network needs to be formed inside the material. This puts forward strict requirements for the microstructure of carbon materials. Conductive carbon black and activated carbon, as zero-dimensional granular materials, are difficult to form high-conductivity pathways within the composite material. Graphene and carbon nanotubes can form a continuous path with high conductivity due to their own structural advantages, especially in the process of composite with cellulose. Therefore, graphene and carbon nanotubes have been widely used in the preparation of 2D cellulose-based Joule thermal devices.

2.2.1.1. 2D cellulose/graphene composite materials. Graphene is a two-dimensional carbon material with excellent conductivity, ultra-high specific surface area, and good thermal conductivity. At present, thanks to its unique two-dimensional structure, graphene has been widely used in energy storage, sensing, electromagnetic shielding, joule heating, and other fields [76–78]. However, due to the strong van der Waals forces and  $\pi$ - $\pi$  bonding forces between two-dimensional graphene nanosheets, direct use of them in the preparation of Joule heating devices will result in serious stacking effects. This affects the service life of graphene-based flexible electric heating devices. Nanocellulose is a one-dimensional material with a large aspect ratio and excellent mechanical properties. By evenly dispersing graphene and nano cellulose in the solute, it can effectively prevent the stacking of graphene nanosheets to form a good conductive path. Li et al. [79] prepared nano cellulose (NFC)/Graphene (GR) composite electric heating membrane through vacuum filtration. Thanks to the dispersion effect of NFC on GR nanosheets, a stable stacking structure of GR nanosheets is formed within the composite membrane. This ensures that the NFC/GR composite film has flexibility, uniform conductivity, and heating performance. The results showed that at a power of  $2000 \text{ W m}^{-2}$ , the NFC/GR composite film reached an electric heating temperature of  $60^\circ\text{C}$  within 3 min. And with the increase in power density and graphene content, the electric heating performance of the composite film also improved. In this work, nano cellulose/graphene composite membrane was used for electric heating performance for the first time, providing a basic reference for the development of biomass-based electric heating materials. However, nanocellulose with a large number of hydroxyl and carboxyl groups can form a large number of hydrogen bonds during the self-assembly process [80]. However, there is still significant room



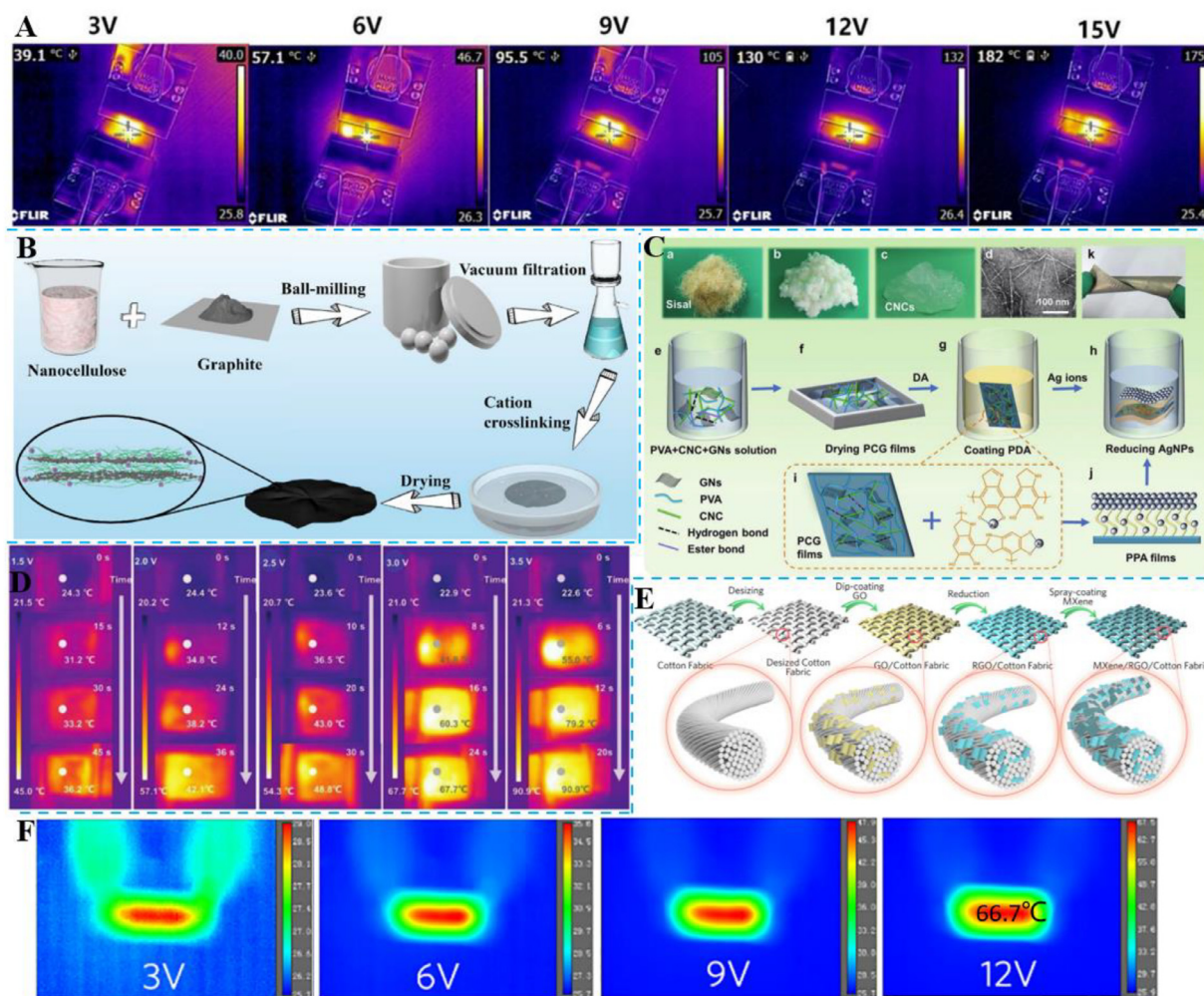


**Fig. 6.** (A) Temperature thermal imaging of cellulose/GO composite material under different voltages [81]. (B) The preparation process of cationic cross-linked cellulose/GO composite membrane [82]. (C) The preparation process of PPA composite membrane. (D) Temperature thermal imaging of PPA composite films under different voltages [83]. (E) The preparation process of RMC composite materials. (F) Temperature thermal imaging of RMC-4 under different voltages [84].

for improvement in its mechanical properties. Tan et al. [81] obtained cellulose/GO composite materials by fully crosslinking cellulose with GO nanosheets using silane coupling agents. The results indicate that the composite film exhibits a tensile strength of 113 MPa. This is mainly because vinyl Trimethoxysilane forms a Covalent bond structure between cellulose and GO, which greatly increases the mechanical properties of the composite. In addition, cellulose/GO composite materials also exhibit excellent electrical heating performance. As shown in Fig. 6(A), the composite material exhibits a thermal response of 39.1–182 °C under an applied voltage of 3–15 V. Similarly, Yang et al. [82] used cation ( $\text{Al}^{3+}$ ,  $\text{Ga}^{2+}$ ,  $\text{Cu}^{2+}$ ,  $\text{Fe}^{3+}$ ,  $\text{Na}^{+}$ , and  $\text{Zn}^{2+}$ ) crosslinking to improve the conductivity and mechanical properties of cellulose/GR composite membranes (Fig. 6(B)). Taking  $\text{Cu}^{2+}$  crosslinking as an example, the crosslinked composite film exhibits a tensile strength of 64.3 MPa. However, the influence of different cationic crosslinking on the Joule thermal properties of composite materials is relatively complex. Ionic radius, cation valence, and thermal conductivity all affect the joule thermal properties of different cross-linked composites. Overall, the composite materials crosslinked with cations exhibit excellent electrical heating performance. This work provides a certain reference for the preparation of cationic crosslinking in 2D cellulose-based Joule thermal materials.

Compared with metal materials, the electric heating performance of carbon materials is slightly inferior. Introducing

metal materials into cellulose/GO composites has become a method to improve conductivity and Joule thermal properties. Li et al. [83] introduced metal silver particles with high conductivity on the surface of polyvinyl alcohol (PVA)/Graphene nanoflake (GN)/nanocellulose crystal (CNC) composite membrane (PCG) through in-situ growth to obtain PPA composite membrane. Fig. 6(C) shows the preparation process of the PPA composite membrane. Thanks to the synergistic effect of GN and the high conductivity of metallic silver particles, PPA composite films exhibit excellent electrothermal properties. As shown in Fig. 6(D), the composite film exhibits a heating performance of 36.2–90.9 °C under an applied voltage of 1.5–3.5 V. And the PPA composite film also exhibits excellent sensing performance. In addition to silver particles, the highly conductive 2D nanosheets MXene are also used to improve the electrothermal properties of cellulose/Graphene composites. Zheng et al. [84] prepared a multifunctional conductive cellulose fabric for electric heating, energy storage, sensing, and electromagnetic shielding through spraying and impregnation. Fig. 6(E) shows the preparation process of the multifunctional conductive fabric. Firstly, the cellulose fabric is pre-treated with NaOH to increase its wettability. Then, RGO/Cotton fabric composite materials are obtained through impregnation and reduction. Finally, MXene/RGO/Cotton fabric (RMC) composite material was obtained through spraying. In this type of work, the author improves the electrical heating performance of the composite

material by increasing the frequency of MXene spraying. As shown in Fig. 6(F), the RMC-4 composite material sprayed four times exhibits an electrical heating performance of 66.7 °C under an applied voltage of 12 V. In addition, RMC-4 also exhibits an electromagnetic shielding performance of 29.04 dB and an energy storage performance of 258 mF cm<sup>-2</sup>.

**2.2.1.2. 2D cellulose/carbon nanotube composite materials.** Carbon nanotubes are a one-dimensional nano highly conductive material with a microtubular structure [85]. And it has excellent aspect ratio, thermal conductivity, and mechanical properties. In the field of electric heating, CNTs can form stable conductive networks. The mechanical properties of the device obtained by using CNT alone in 2D film materials are poor, and the agglomeration effect of CNT can also cause uneven heat dissipation in the device. So it is particularly important to seek a spacer between CNTs. The use of cellulose as a mechanical reinforcement and spacer for CNTs is an excellent method for preparing electric heating devices with excellent mechanical properties. Li et al. [86] prepared CNT/nano cellulose (NFC) composite Heating film by vacuum filtration. And use polydimethylsiloxane (PDMS) for encapsulation. The CNT/NFC composite film has an electrical heating performance of 60.7 °C at a voltage of 7.8 V. In addition to using PDMS as a mechanical reinforcement and packaging material, its thermal expansion performance can also be utilized to prepare electrothermal-based soft weightlifting materials. Ghosh et al. [87] designed a layered structure based on cellulose to achieve an electric heating actuator. Fig. 7(A) shows the preparation process of the composite material. Firstly, CNT is loaded onto the surface of cellulose paper through vacuum filtration to form a double-layer structure. Then, PDMS polymer is coated on the surface of CNT to form a three-layer structure through spin coating. Finally, the obtained composite material is cut into a “U” shape to obtain an electric heating actuator. To ensure sufficient conductivity of CNT in the electric heating material, conductive epoxy resin is used to fix the fine copper wire with the intermediate layer CNT. Fig. 7(B) shows the working schematic diagram and corresponding optical images of the electric heating actuator. The electric heating energy generated by the CNT layer under external voltage is controlled by the thermal expansion of PDMS and the wet expansion of cellulose paper to achieve stable operation of the actuator. In addition, this work also discussed the working ability of the actuator under different voltages. In summary, this work utilizes the energy generated by electric heating and the properties of the materials (PDMS and cellulose) themselves to construct an electrothermal actuator. This has opened up the design concept of paper-based electric heating actuators, providing guidance for the multifunctional application of paper-based electric heating devices. The large-scale preparation is crucial for the future development of cellulose-based electrothermal materials. As a very mature industrial product, the papermaking process can be applied to the preparation of cellulose paper-based electric heating devices to achieve stable large-scale preparation. As shown in Fig. 7(C), Yang et al. [88] prepared a flexible electrically heated paper-based composite based on CNT/poly (isophthaloil M-Phenylenediamine) (CNT/PMIA) using a papermaking process. By controlling the content of CNT, paper-based composite materials with different active substance contents are obtained. Considering the working temperature of PMIA and the stability of the composite material, the CNT/PMIA composite paper obtained with a CNT content of 30 % exhibits the most excellent electrical heating performance. In addition, the paper-based material also shows stable electrothermal performance (Fig. 7(D)) after 100 cycles of opening and closing, with highly stable heating capacity and uniform temperature distribution. In order to optimize the dispersion of CNT in the papermaking process of pulp in this process, Yang's group

[89] carboxylated CNT to obtain a stable conductive pulp dispersion. In addition, CNTs treated with carboxylation can also form strong forces with PMIA fibers, thereby improving the mechanical properties of conductive paper. As shown in Fig. 7(E), the composite material can reach an electric heating temperature of 242 °C under a safe voltage of 25 V. In summary, these two works have achieved large-scale preparation of PMIA fiber/CNT paper-based electrothermal composite materials using mature papermaking processes. From the perspective of industrialization, these two tasks have certain practical value.

In the field of flexible electronics, wearable intelligent conductive fabrics also have certain application potential. As shown in Fig. 8(A), Chen et al. [90] prepared 1D holocellulose nanofibrils /carbon nanotubes/cellulose aerogel fibers (HCCAFs) based on CNT through wet spinning and then prepared 1D composite fibers into 2D HCCAFs conductive fabrics through the weaving process. As shown in Fig. 8(B), the conductive yarn after three-step coagulation bath treatment has a clear 3D porous network structure. This also fully indicates the formation of a uniform and stable structure between cellulose and CNT, avoiding the aggregation of CNTs. Thanks to the porous conductive structure, the conductive fabric exhibits an electric heating temperature of 179.6 °C at a low voltage of 2.5 V. The porous conductive structure also endows 2D-HCCAFs conductive fabrics with excellent electromagnetic shielding performance, with an EMI shielding performance of 32–65 dB at a thickness of 0.21 to 0.72 mm. In addition, the prepared conductive textiles also exhibit excellent washing resistance and durability, which ensures the stability of the textiles in practical applications. High-conductivity MXene materials are also used to enhance the electrothermal performance of cellulose/CNT composite films. As shown in Fig. 8(C), Zhang et al. [91] prepared a layered conductive network structure using dip coating and spray coating methods CNT@MXene/Cellulose membrane (CNT@MXene/CF). Firstly, MXene is impregnated multiple times to obtain MXene/CF. Then spray the configured CNT ink onto its surface to obtain CNTs@MXene/CF. Due to the presence of a large number of hydroxyl groups between the three, a strong interlayer binding force is formed through hydrogen bonding. As shown in Fig. 8(D), CNT@MXene/CF has an electric heating performance of 156 °C at a voltage of 4 V. And the composite material showed stable electric thermal conversion performance after 20 on-off cycles under constant voltage.

### 2.2.2. 2D cellulose/metal composite materials

Metal materials have been widely used in various fields of life due to their excellent conductivity [92]. In cellulose-based electric heating composite materials, metal materials such as MXene, Ag [93], Fe [94], and Ni [95] are also combined with cellulose through vacuum filtration, in-situ growth, impregnation, and spraying. This section summarizes cellulose/metal Joule thermal composite materials by categorizing different metal types.

**2.2.2.1. 2D cellulose/MXene composite materials.** In recent years, the unique physical and chemical properties and unique two-dimensional conductive structure of MXene materials have attracted widespread attention in the fields of energy storage, sensing, and Joule heating. Kim et al. [96] obtained two types of cellulose-based electrothermal composite materials by impregnating MXene onto cellulose paper and fabric. The MXene/cellulose paper (MCPs) and MXene/fabric (MCFs) obtained through repeated impregnation and drying exhibited conductivity of 1.91 and 0.05 S cm<sup>-1</sup>, respectively. MCPs exhibit a heating temperature of 210 °C at a voltage of 15 V. MCFs have a thermal performance of 180 °C at a voltage of 30 V. This is mainly due to the continuous high conductivity network formed by MXene nanosheets on



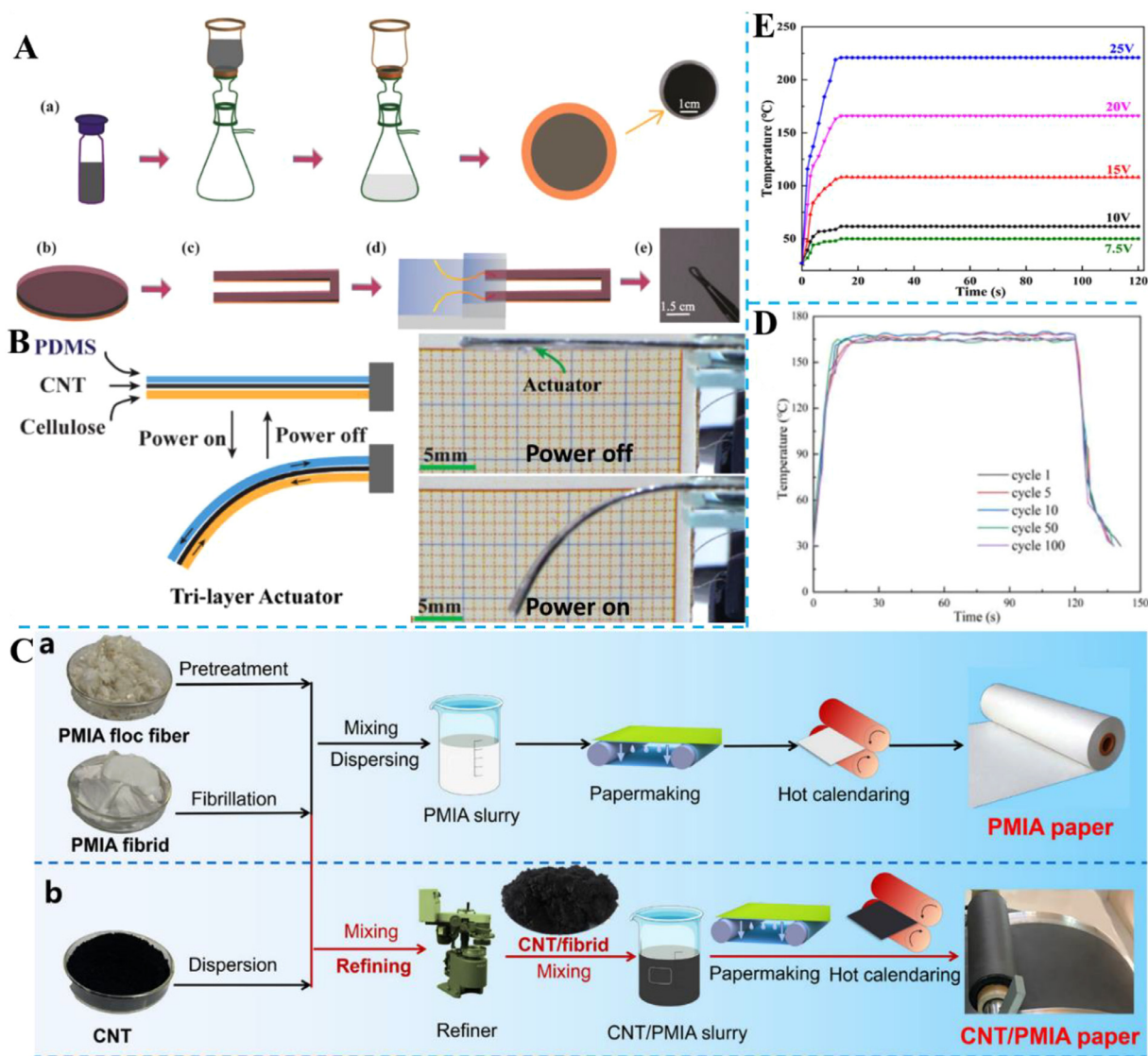


**Fig. 7.** (A) Preparation process of the cellulose-based electrothermal actuator. (B) Schematic diagram of the actuator and its corresponding physical image [87]. (C) The preparation process of CNT/PMIA paper-based electric heating materials. (D) Cyclic stability performance test of CNT/PMIA electric heating [88]. (E) Electric heating curves of CCNT/PMIA at different voltages [89].

the surface and inside of cellulose laminated materials, providing channels for high-speed electron transfer and generating effective heat. Similarly, Zhao et al. [97] also prepared conductive cellulose fabrics based on MXene using the impregnation process (Fig. 9(A)). The composite material exhibits a heating performance of 100 °C at a voltage of 6 V. And the generated heat can be evenly distributed around the injured skin to accelerate wound healing. This cellulose-based Joule thermal device has great application prospects in portable medical devices. In order to enhance the electrical heating performance of MXene-based conductive fabrics, conductive fabrics coated with metal silver particles were obtained through in-situ growth [98]. Finally, the silver and MXene bimetallic matrix electrically heated composite fabric was obtained by coating MXene on the surface through impregnation. This composite material exhibits excellent Joule thermal performance and photothermal shape-driving performance.

Vacuum filtration is the most common preparation method for cellulose/MXene composite materials. Compared with the original MXene film, due to the strong hydrogen bonding force between cellulose and MXene, a pearl-like layered structure can be formed. The toughening effect of this structure, similar to the

“brick and mortar” structure in architecture, ensures the mechanization. Through self-assembly between BF and bonding between BF and MXene, mechanical properties of MXene-based composite materials [99]. As shown in Fig. 9(B), Zhu et al. [100] prepared MXene/Bamboo textile (BF) composite paper-based materials through simple vacuum filtration. MXene/BF composite materials exhibit a tensile performance of 49.5 MPa, which is much higher than that of pure MXene and BF-prepared membrane materials. In addition, MXene/BF also exhibits a high conductivity of  $4800 \text{ S m}^{-1}$ . In order to increase the lifespan and comfort of paper-based materials used in flexible wearable devices, MXene/BF paper-based electric heaters were obtained through PDMS encapsulation. At a low voltage of 3 V, the heating device can reach a temperature plateau of 65.3 °C within 180 s. The cellulose/MXene composite material used for flexible Joule heating equipment should not only have a certain degree of electric heating ability but also have certain antibacterial properties. This can maximize human health and safety while using cellulose-based electrothermal materials for flexible wearable devices. As shown in Fig. 9(C), Wei et al. [101] prepared a CNF/MXene-TA composite paper with both Joule heat and antibacterial properties by adding tannic acid (TA). In addition, compared



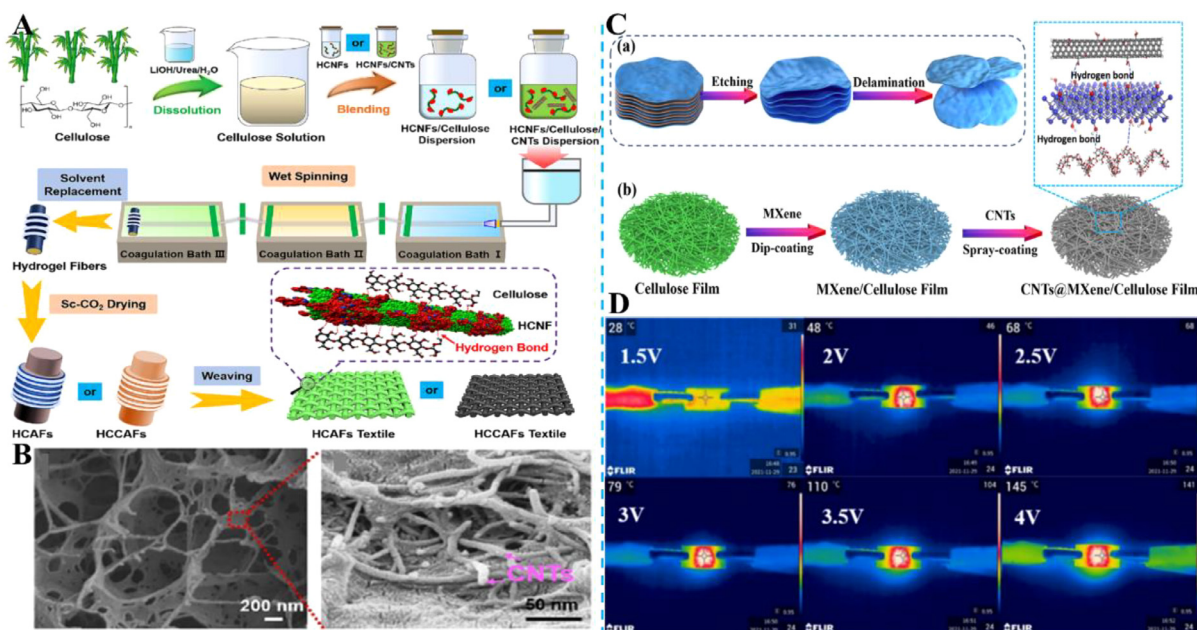


**Fig. 8.** (A) Schematic diagram of the preparation of HCCAFs fabric. (B) Cross-section SEM images of HCCAFs [90]. (C) Schematic diagram of the preparation process of CNT@MXene/CF. (D) Temperature infrared images of CNT@MXene/CF under different voltages [91].

to paper-based materials without TA (245 MPa), the addition of TA greatly enhances the mechanical properties of paper-based materials. CNF/MXene-TA composite paper exhibits a super strong tensile performance of 275 MPa. The author suggests that the improvement in mechanical properties is mainly attributed to the hydrogen bonding crosslinking between CNF and MXene, as well as the plasticizing mechanism of TA. It is worth noting that the addition of TA will have a certain impact on the conductivity of paper-based materials. In this work, the author selected the optimal usage ratio of TA by considering the effects of mechanical strength and electric heating response. The results showed that CNF/MXene TA composite paper exhibited stable Joule thermal properties. Under 5 V voltage, the heating temperature is kept constant for 6000 s, showing excellent stability and practicability as a personal thermal management device. In addition, polyethylenimine (PEI) and polydopamine (PDA) are also used to improve cellulose/MXene paper-based electrothermal materials. As shown in Fig. 9(D), Zhou et al. [102] prepared a composite paper-based material (CMP) with a “mortar” structure of MXene and cellulose nanofibers by adding PEI. Thanks to the significant electrostatic interaction between  $\text{NH}_3^{3+}$  groups on the PEI molecular chain and negatively charged MXene nanosheets, CMP paper-based materials exhibit tensile properties of 140 MPa. Thanks to its excellent mechanical and electrical properties, CMP can rise to 100.14 °C under a voltage of 9 V within 8 s. In addition, CMP membranes also exhibit excellent degradability. In a concentration of 1 wt%  $\text{H}_2\text{O}_2$  solution, the CMP membrane can be completely degraded within 14 days. Zhang et al. [103] obtained a paper-based composite material with a pearl shell structure by alternating vacuum filtration of PDA-modified MXene nanosheets and bacterial cellulose (BC). The ultrafine network structure of BC provides a strong and tough skeleton structure for composite materials. In addition, while not sacrificing the conductivity of MXene, the mechanical properties and stability of MXene nanosheets modified with PDA have been improved to a certain extent. At a voltage of 6 V, the heating performance of the composite material reaches 85 °C (Fig. 9(E)). From the above work, it can be seen that the introduction of crosslinking agents and surface modification can effectively increase the mechanical properties of cellulose/MXene composite electrothermal materials. This is particularly

important for the development of high-performance 2D cellulose-based electrothermal materials. In addition to vacuum filtration, which can deeply crosslink cellulose with MXene, the coating process can also achieve deep crosslinking between cellulose and MXene. Wang et al. [104] obtained ANF/MXene composite conductive paper through scraper coating and sol-gel steps. As shown in Fig. 9(F), first coat ANF/MXene dispersion liquid through a scraper to form a uniform hydrogel. Then, ANF/MXene composite paper was obtained by freeze-drying. As shown in Fig. 9(G), at a lower voltage, the infrared thermal image of the composite paper exhibits a uniformly distributed heat distribution and a higher heating temperature. And the composite paper still maintains a stable heating temperature after prolonged operation for 1500s, exhibiting stable Joule thermal performance.

**2.2.2.2. 2D cellulose/silver composite.** The work of 2D cellulose/metal Joule thermal devices, due to the excellent conductivity and antibacterial properties of metal silver, has attracted extensive attention in the preparation of 2D cellulose-based Joule thermal devices. Antibacterial properties are very important for the practical application of personal thermal management devices. This can not only ensure the healthy application of electric heating to the human body but also protect the human body from foreign harmful bacteria. Metallic silver can be divided into zero-dimensional silver nanoparticles [105] and one-dimensional silver nanowires [106] in the preparation of electric heating materials and devices. The main preparation processes of cellulose/silver nanocomposites are coating, sputtering, and in-situ growth. The preparation method of cellulose/silver nanowire composites is mainly vacuum filtration. Yue et al. [107] coated CNT and Ag conductive layers on cellulose paper by polishing process and magnetron sputtering to obtain cellulose/cnt/ag electrothermal materials (CCA) with double-layer conductive structure. Fig. 10(A) shows the preparation process of the CCA composite and its corresponding structural diagram. As shown in Fig. 10(B), the CCA film can reach a temperature of 48 °C at an applied voltage of 3.7 V at room temperature of 15 °C. It is obvious that the heat is evenly distributed on the surface of the composite, which is mainly due to the high conductivity of the Ag layer. In addition, the surface treatment of paper-based materials to in-

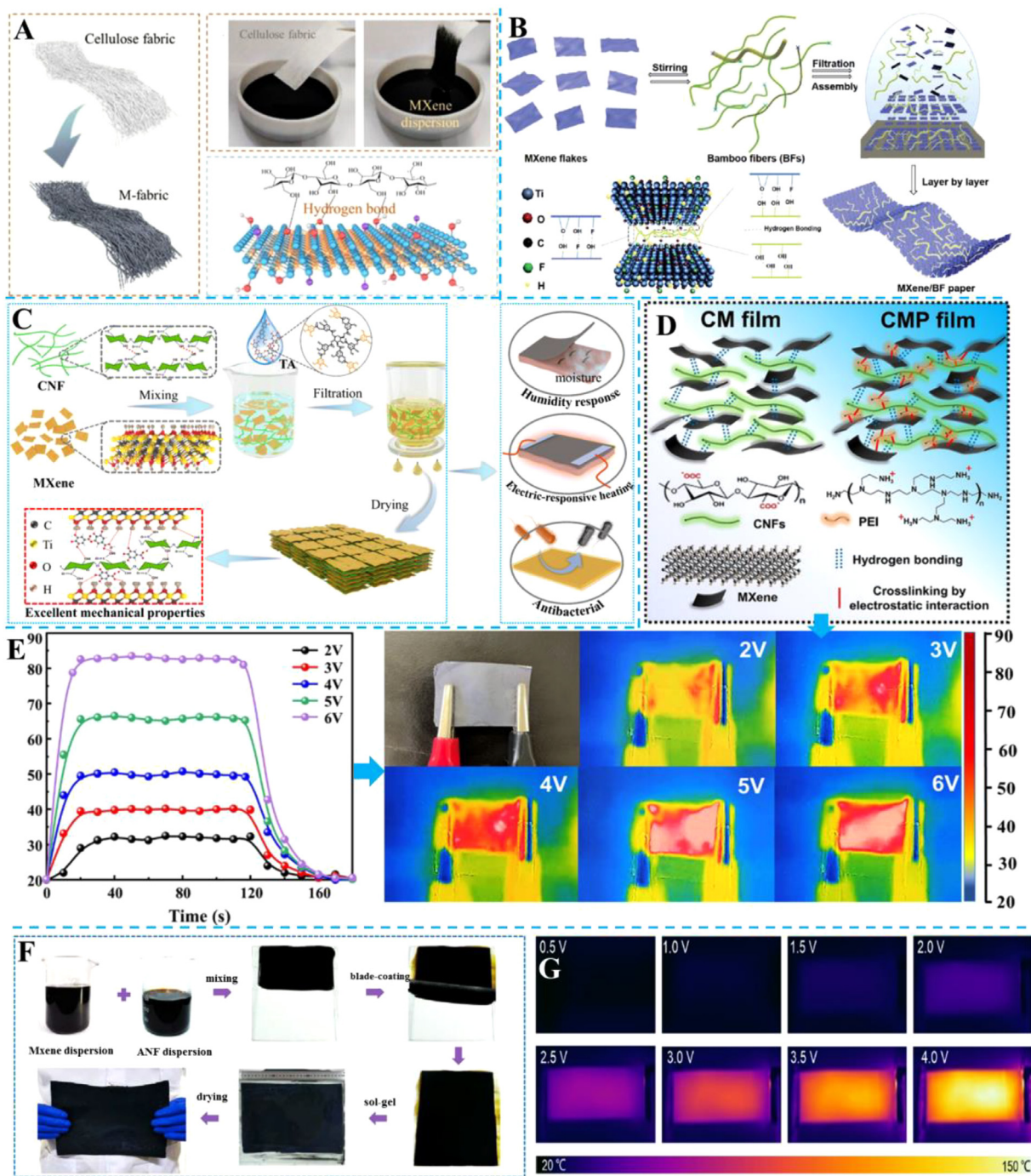


**Fig. 9.** (A) schematic diagram of preparation of conductive cellulose fabric based on MXene [97]. (B) The preparation process of MXene/BF [100]. (C) The preparation process of CNF/MXene Ta Composite paper [101]. (D) Schematic diagram of the CMP preparation process [102]. (E) The Joule thermal performance of CMP under different voltages and its corresponding infrared temperature image [103]. (F) MXene/ANF composite paper preparation process. (G) The infrared temperature images of MXene/ANF under different voltages [104].

crease their roughness and thus increase the close load of conductive materials is also used in the preparation of paper-based thermoelectric materials. As shown in Fig. 10(C), Zhu et al. [108] increased the surface roughness and oxygen content of aramid paper (AFP) by plasma treatment in order to improve the tightness of the Metal Ag conductive layer on the material surface. After treatment, the surface of AFP is rich in oxygen-containing functional groups, which increases the interaction with the Ag layer. The load of the conductive Ag layer gives AG/AFP the ability to convert electrical energy into thermal energy. As shown in Fig. 10(D), the composite paper sputtered with metal Ag for 4 min has excellent electri-

cal heating performance at a load voltage of 0.5–1.5 V. In addition, increasing the sputtering time of the Ag layer can also effectively increase the Joule thermal properties of composite paper. Similarly, Zhou et al. [109] deposited uniform metallic silver nanoparticles on the surface of plasma-treated AFP by in-situ growth. As shown in Fig. 10(E), the AFP surface after plasma treatment has added many rough sites after corrosion, which provides more active sites for the growth of metallic silver particles. In addition, the surface of the composite after in-situ growth has closely connected metallic silver particles, which provides sufficient electrical conductivity for the composite. At a voltage of 1 V, its maximum temperature



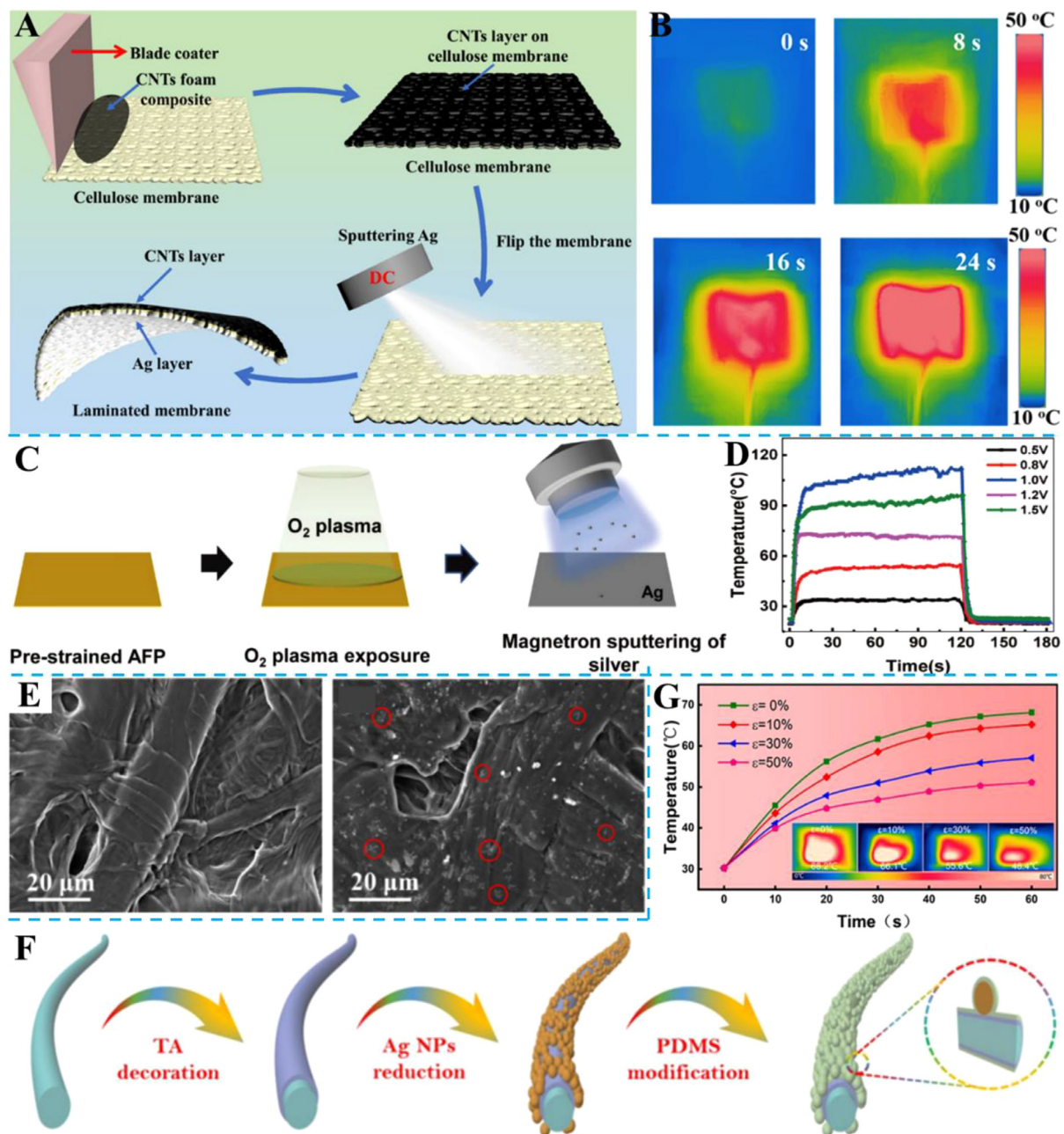


**Fig. 10.** (A) CCA preparation process. (B) Thermal imaging of CCA at different voltages [107]. (C) Schematic diagram of AG/AFP preparation. (D) Temperature time curve of AG/AFP [108]. (E) SEM images of AFP and plasma-treated AFP [109]. (F) Schematic diagram of the preparation process of cotton/TA/AgNPs/PDMS conductive fabric. (G) Joule thermal property curves of conductive fabrics under different tensile states [110].

reached an amazing 210 °C. This is far lower than the safe voltage of human contact and has great application value in the field of flexible electric heating devices. With the rapid development of flexible electronic equipment used in the human body, intelligent textile clothing has also attracted extensive attention. Guo et al. [110] obtained multifunctional intelligent cellulose textile fabrics for Joule heat, antibacterial, sensing, and antifouling properties by in-situ growth of metallic silver on cotton fibers. Fig. 10(F) is a flow chart for the preparation of the textile cloth. First of all, Tannic acid (TA) was used to modify the surface of cellulose fabric to increase the adsorption capacity of metal silver particles. Then the conductive fabric was obtained by the reduction growth of metallic silver particles. Finally, in order to enhance its antifouling ability and mechanical properties, PDMS was used to package it to obtain multi-

functional cotton/TA/AgNPs/PDMS conductive fabric. Under the applied voltage of 0.5–1.5 V, the saturation temperature of textiles reached 36.5–73.6 °C. When the voltage reached 2 V, the heating temperature of the textile reached 118.7 °C. In addition, the conductive fabric also has excellent tensile properties when used in electric heating devices. As shown in Fig. 10(G), the electrothermal temperature retention rate of conductive fabric is 70 % when the tensile degree is as high as 50 %.

Compared with metallic silver nanoparticles, silver nanowires (AgNWs) have a larger aspect ratio and excellent mechanical properties. Ma et al. [111] prepared aramid nanofibers (ANF)/AgNWs conductive multifunctional electric heater by two-step vacuum filtration. As shown in Fig. 11(A), ANF/AgNWs layered composite materials can be obtained by passing ANF and AgNWs through two



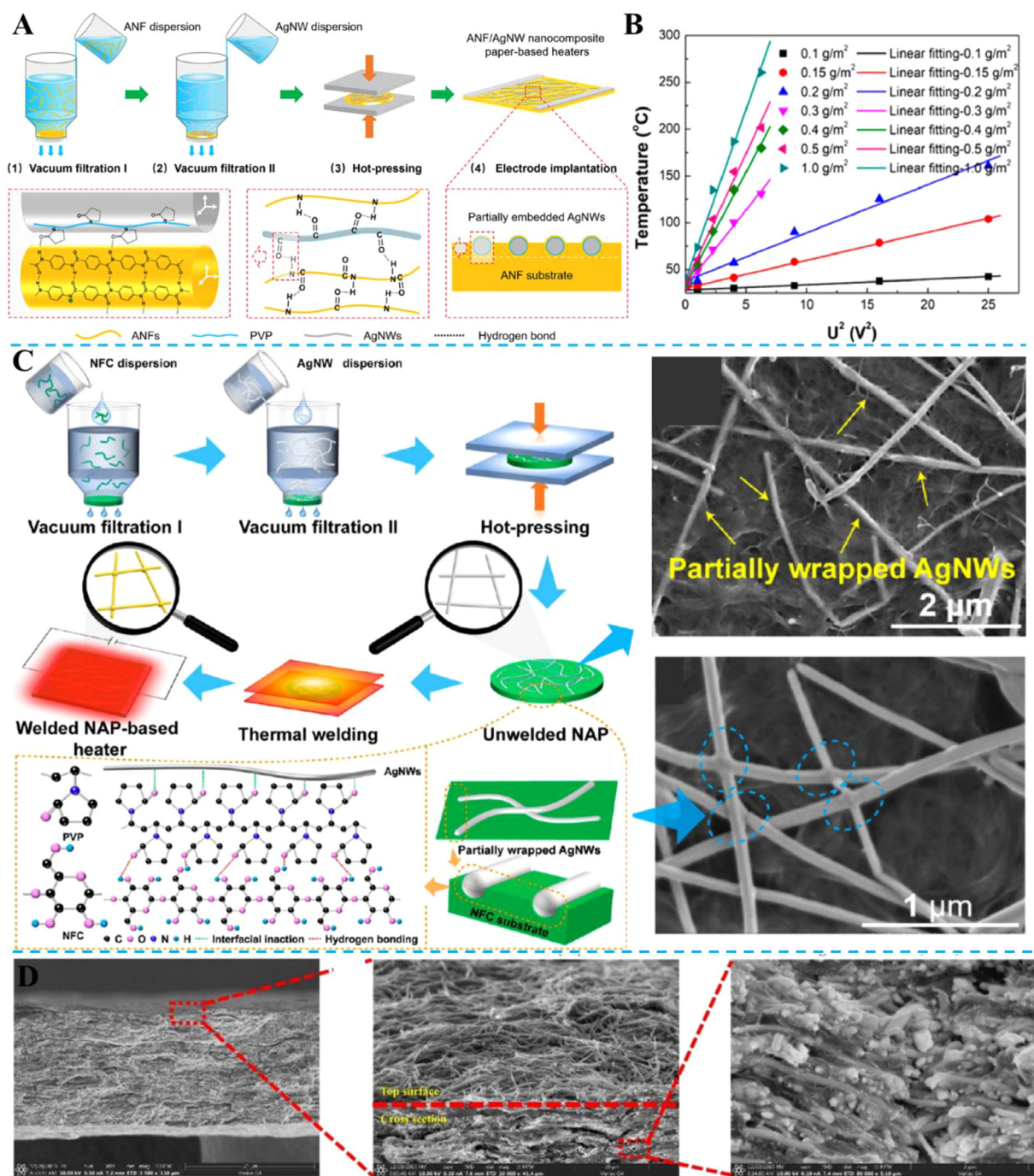


**Fig. 11.** (A) Schematic diagram of the preparation process of ANF/AgNWs layered composite material. (B) The Joule thermal performance of composite materials with different AgNWs loading levels under different driving voltages [111]. (C) Schematic diagram of the preparation process of NAP-based electric heating devices and their corresponding microscopic morphology images [112]. (D) SEM images of the cross-section of cellulose/AgNWs composite materials [113].

rounds of vacuum filtration and hot pressing. Due to the large number of hydrogen bonds between ANF and AgNWs, the layered structure shows excellent adhesion. ANF/AgNWs composites with different loading contents were obtained by controlling the amount of AgNWs used in the vacuum filtration process. It can be seen from Fig. 11(B) that with the continuous increase of load, a higher heating temperature can be achieved at a lower voltage. In addition, the electric heating performance of ANF/AgNWs also maintains good stability under different bending angles. Similarly, Cheng et al. [112] used nanofibrous cellulose (NFC) as the substrate to wrap a small part of AgNWs in the NFC layer by vacuum filtration and hot pressing to obtain NFC/AgNWs paper (NAP)

(Fig. 11(C)). Thanks to the synergy between NFC substrate and AgNWs after hot press welding, NAP paper showed excellent flexibility and 176 MPa mechanical tensile strength. And it has a Joule thermal property of over 220 °C. In this work, the author realized the large-scale preparation of NAP paper-based functional materials by spraying. This also shows that the spraying process can realize the large-scale preparation of layered paper-based functional materials. With the large-scale use of wireless devices, electromagnetic radiation also affects people's health in life. Therefore, it is particularly important to integrate EMI shielding performance into electrothermal materials in the preparation of electrothermal devices. Liang et al. [113] designed a bifunctional cellulose/AgNWs

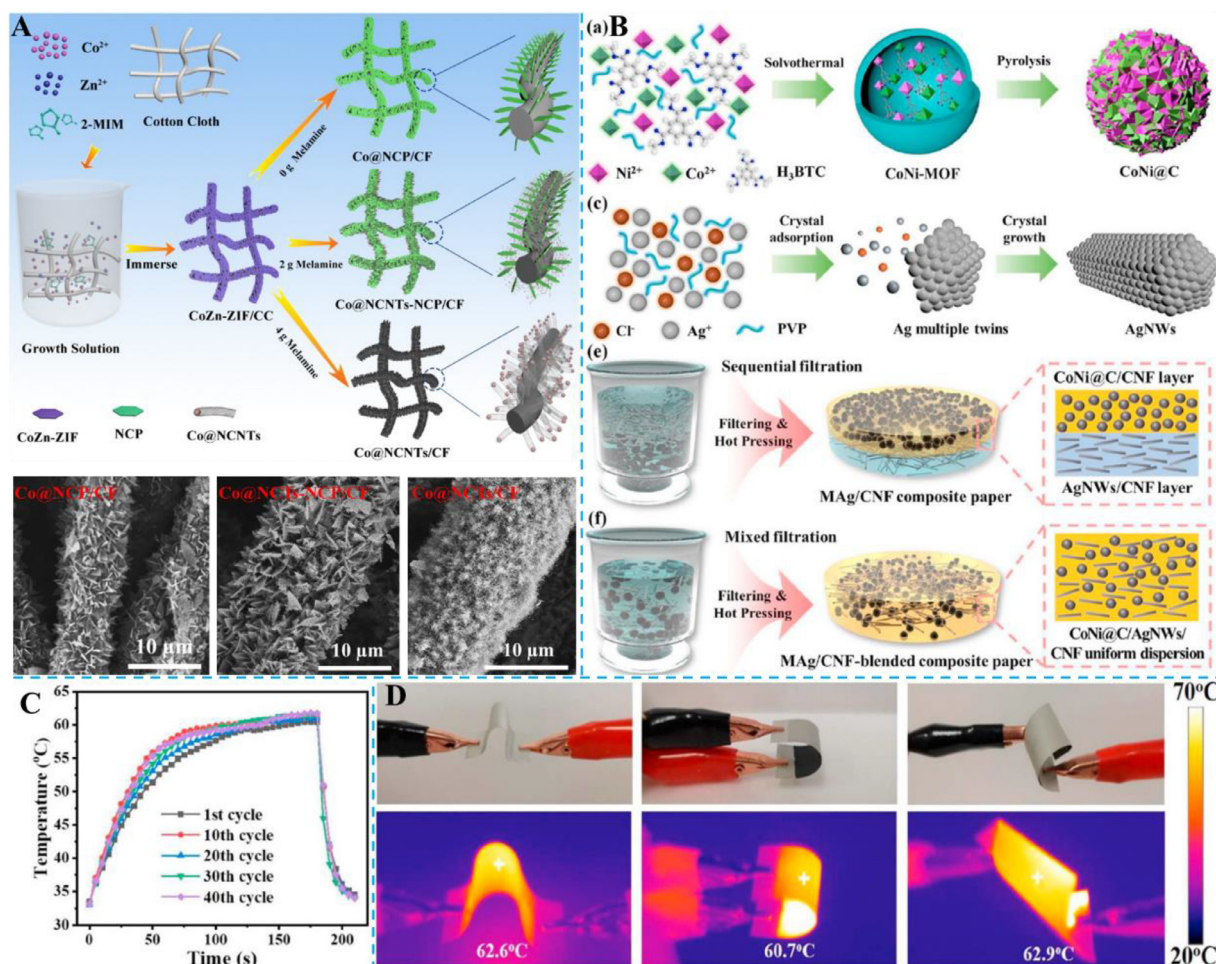


**Fig. 12.** (A) Preparation process of cellulose-based composite material loaded with cobalt nanoparticles and N-doped CNT [115]. (B) Preparation process of MAG/CNF composite material. (C) Cyclic stability of MAG/CNF electrothermal performance. (D) Infrared thermal imaging of MAG/CNF with different bending angles under constant voltage [116].

composite paper-based film with high-performance EMI shielding and Joule thermal performance integration. Fig. 11(D) shows the cross-sectional SEM image of the cellulose/AgNWs membrane. Due to the cross-linking between cellulose and AgNWs and hot pressing treatment, the composite membrane showed a uniform and dense structure. This is conducive to the formation of a continuous high-conductivity network ( $5517 \text{ S m}^{-1}$ ) inside the composite. This material has an EMI shielding performance of 101 dB at a thickness of 45  $\mu\text{m}$ . And it has a heating performance of 99.5  $^{\circ}\text{C}$  at 2 V low pressure. Therefore, cellulose/AgNWs composite electrothermal paper can be driven by simple energy storage devices such as common dry batteries or even flexible energy storage supercapacitors. Similarly, Lv et al. [114] prepared cellulose-based electrothermal composites by pouring AgNWs and natural silk fibers and vacuum filtration. Thanks to the synergy between AgNWs and cellulose filaments, the composites exhibit excellent flexibility, folding resistance, and rapid electrothermal response.

**2.2.2.3. 2D cellulose/other metal composite materials.** In addition to MXene and Ag (AgNWs), there are also many metal materials used for Joule heating, such as iron, nickel, cobalt, and manganese and their compounds. Zhang et al. [115] loaded cobalt nanoparticles embedded in N-doped CNT multifunctional composites on carbonized cotton fiber cloth through in-situ growth. Fig. 12(A) shows the preparation process of the composite material. Firstly, cotton fiber cloth (CC) was soaked in a precursor

solution of metal growth to obtain  $\text{CoZn-ZIF/CC}$  composite material. Then three kinds of Metal matrix composite were obtained by controlling the content of melamine. Three different morphologies of composite materials are named  $\text{Co@NCP/CF}$  (0 g melamine),  $\text{Co@NCNTs-NCP/CF}$  (2 g melamine), and  $\text{Co@NCNT/CF}$  (4 g melamine). From the corresponding SEM images, it can be seen that as the amount of melamine used increases, the number and density of NCNT growth also increase. In the applications of absorption and electric heating,  $\text{Co@NCNT/CF}$  exhibits excellent absorption performance and Joule thermal performance. This is mainly due to the synergistic effect between NCNT and Co. It exhibits a Joule heating temperature range of 39.5–160.2  $^{\circ}\text{C}$  under an applied voltage of 1–2.5 V. The composite material obtained from carbonized cellulose inevitably leads to a decrease in mechanical properties. The non-carbonized composite material prepared by blending metal materials with cellulose through vacuum filtration can maintain excellent mechanical tensile properties. As shown in Fig. 12(B), Liang et al. [116] prepared two structures through vacuum filtration  $\text{CoNi@C/AgNWs/CNF}$  paper-based electrothermal materials (MAG/CNF). Firstly, it was prepared by hydrothermal and carbonization methods  $\text{CoNi@C}$  Metal nanospheres. Then one-dimensional linear rigid AgNWs were prepared. Finally, the laminated MAG/CNF composite paper and the uniform structure composite paper were prepared by different mixing and filtering Rota systems. Thanks to the high conductivity of the layered structure and effective EMI shielding structure, this material ex-



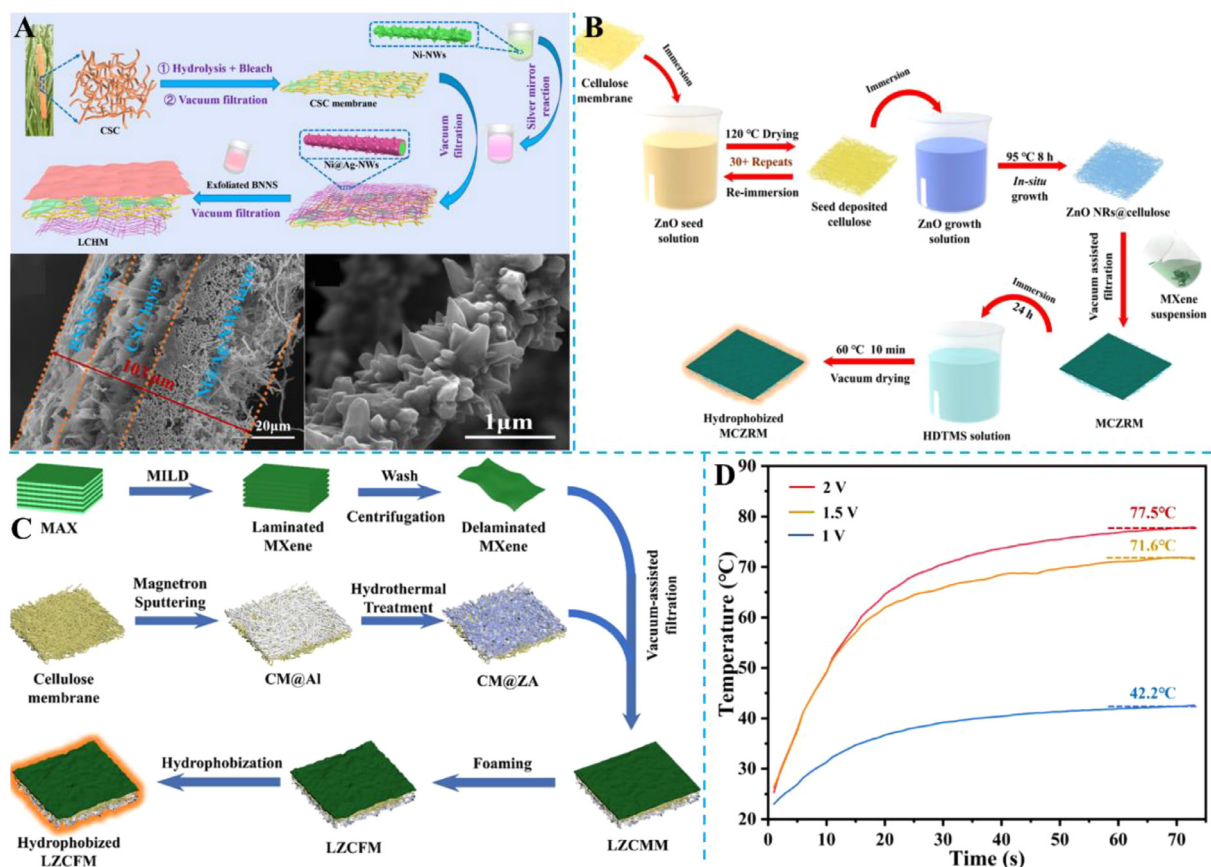


**Fig. 13.** (A) Preparation process of LCHM [117]. (B) The preparation process of MXene/cellulose/ZnO composite membrane [118]. (C) Schematic diagram of the preparation process of LZCFM. (D) The Joule thermal performance of LZCFM [119].

hibits excellent electrical and EMI shielding properties. As shown in Fig. 12(C), when the applied voltage is 2.5 V, the heating performance of the composite material reaches 86 °C. And after 40 on-off cycles, it still maintains good electrical heating stability. In addition, thanks to the excellent flexibility of CNF, the heating temperature of MA/CNF composite paper remains almost unchanged at different bending angles (Fig. 12(D)).

In the research work of cellulose/metal electric heating materials, Zhang's group [117–119] from Jiangsu University in China has made some good research content. They successfully applied metals such as Ni, Zn, and Al to cellulose-based electric heating devices using vacuum filtration, in-situ polymerization, and self-assembly preparation methods. As shown in Fig. 13(A), the team used a layer-by-layer self-assembly method to prepare Ni@AgNWs /Cattail stick cellulose (CSC)/boron nitrate nanosheets (BNNS) laminated cellulose composite membrane (LCHM) [117]. Under the cooperation of silver, nickel, and Molybdenum disulfide, the LCHM composite film exhibits a maximum electric heating temperature of 120 °C under 10 V applied voltage. In addition, the team obtained multifunctional devices with radiation thermal management, Joule thermal performance, and EMI shielding performance by designing MXene/cellulose/ZnO composite films with Janus structure (Fig. 13(B)) [118]. ZnO endows the composite film with certain Radiative cooling performance. And MXene endows the composite film with excellent electrical heating performance. Similarly, on the basis of the previous work, the team introduced a metal aluminum layer on the cellulose fiber surface by sputtering and then obtained a laminated MXene foam/cellulose@Zn Al composite film (LZCFM) through hydrothermal and foaming processes (Fig. 13(C)) [119]. At lower voltages, LZCFM also exhibits good Joule thermal

performance (Fig. 13(D)). In summary, these works have prepared polymetallic cellulose-based composites with excellent Joule thermal properties. This provides a certain reference for the application of multi-metal composite materials in the field of Joule heating.

### 2.2.3. 2D cellulose/conductive polymer composite materials

2D cellulose materials (such as cellulose textiles and cellulose paper) have a large specific surface area and abundant chemical groups, providing sufficient space for the loading of conductive polymers. Jalil et al. [120] loaded continuous PEDOT: PSS conductive polymer onto the surface of cotton fabric through impregnation. As shown in Fig. 14(A), through multiple impregnation drying processes, a uniform load of conductive polymers was achieved on the surface of cotton fabric, forming a continuous conductive network. At a high voltage of 40 V, the composite material exhibits Joule thermal properties at 95 °C. However, the applied voltage of 40 V has exceeded the safe voltage for human contact (36 V). This is mainly due to the difficulty in forming high conductivity of a single conductive polymer on cellulose substrates. Based on this, enhancing the conductivity of conductive polymers through metal materials has been used in the preparation of cellulose-based Joule thermal composites. As shown in Fig. 14(B), Li et al. [121] prepared cellulose/MXene/PEDOT: PSS (CMPC) electrically heated composite materials through vacuum filtration. In this material, MXene greatly improves the conductivity of conductive polymers. Thanks to the synergistic effect between MXene and PEDOT: PSS, CMPC has a thin layer resistance of  $7.2 \Omega \text{ sq}^{-1}$ . Under an applied voltage of 3 V, CMPC has an electrical heating performance of 30 °C (room temperature of 15 °C). Blending MXene nanosheets with conductive polymers to prepare highly conductive inks has also be-



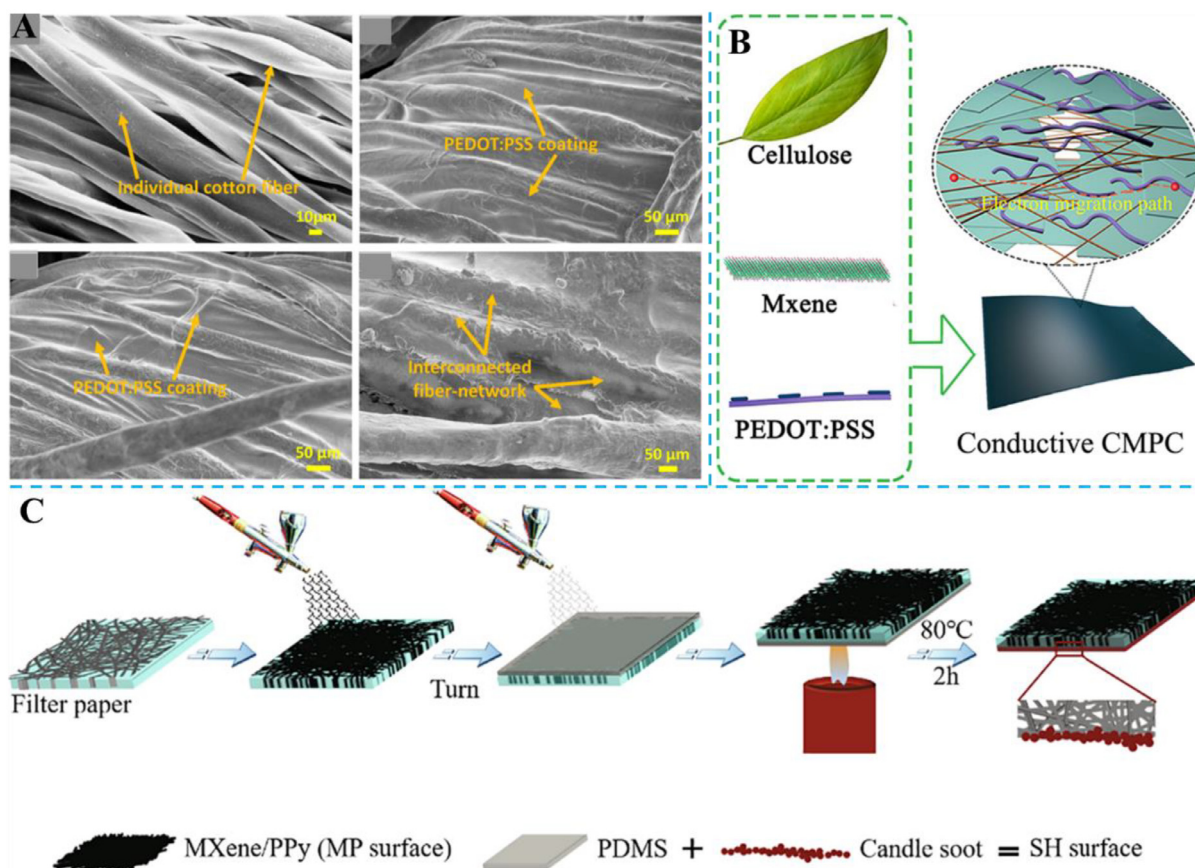


**Fig. 14.** (A) SEM image of conductive fabric [120]. (B) Schematic diagram of the preparation process of CMPC composite membrane [121]. (C) The preparation process of CMP [122].

come a method to improve the conductivity of conductive polymers. Li et al. [122] uniformly coated MXene/Polypyrrole (PPy) ink on the surface of cellulose paper (filter paper) by spraying process to obtain conductive cellulose matrix composites. In order to increase the hydrophobicity of the composite material, a cellulose/MXene/PPy (CMP) multifunctional composite material for Joule heating, nanogenerators, and electromagnetic shielding was obtained by spraying PDMS on the non-conductive layer (i.e. conductive ink spray facing the side) (Fig. 14(C)). Thanks to the uniform loading of highly conductive ink, CMP composite materials exhibit Joule thermal properties of 40–140 °C under an applied voltage of 2–6 V. And from the figure, it can be seen that the emitted heat energy is uniformly loaded on the surface of the composite material. In summary, this work provides a new approach to improving the electrothermal performance and conductivity of cellulose/conductive polymer composites. It also has important reference value for the development of high-conductivity inks in spray-based large-scale preparation processes.

Based on the above summary and discussion of 2D cellulose-based composite Joule thermal composite materials. It can be seen that the research content of 2D cellulose-based electrothermal materials is relatively extensive, and sufficient theoretical research foundation has been obtained. Vacuum filtration, impregnation, sputtering, in-situ growth, papermaking processes, and textile weaving processes are all used in the preparation of 2D cellulose-based composites. In terms of current research, achieving large-scale and stable preparation of cellulose-based electric heating devices still has great research value. Table 2 summarizes the performance parameters of some 2D cellulose-based Joule thermal devices.

### 2.3. 3D cellulose-based composite materials designed for Joule heating

In order to obtain cellulose-based composites with high elasticity, high mechanical strength, and stable electric heating conductive pathways, the preparation of 3D structured electric heating devices through carbonization and composite with other active substances has attracted widespread attention. Generally, the most common types of cellulose-based electrothermal materials based on 3D structure are carbonized wood, cellulose/carbon nanotube Aerogel, cellulose/MXene Aerogel, wood/Graphene, and other composites. Various forms of 3D cellulose-based Joule thermal materials can meet the application needs that cannot be met by 1D and 2D structures in practical applications, for example, compressibility, high elasticity, and other properties. And 3D structured cellulose-based Joule thermal devices can also provide a large heat dissipation area. In recent years, significant research progress has been made in the preparation and application of 3D cellulose-based Joule thermal devices.

#### 2.3.1. 3D cellulose carbon-based composite materials

Wood is a renewable biomass material with an excellent porous structure, which has advantages such as uniform pore structure, easy processing, and high mechanical strength [123]. Thanks to the vertically arranged pore structure and larger pore size, wood has been widely used in the field of electric heating. Zhao et al. [124] prepared bifunctional conductive wood (C-Wood) for EMI shielding and Joule thermal performance using carbonized wood after lignin removal (Fig. 15(A)). The results indicate that C-Wood exhibits the best EMI shielding performance (54.9 dB) and Joule

**Table 2**  
Main performance parameters of 2D cellulose Joule thermal composite materials.

Material	Voltage (V)	Temperature (°C)	Response time (s)	Recovery time (s)	Refs.
NFC/GR	–	60	180	–	[79]
cellulose/GO	15	182	35	10	[81]
cellulose/GR(Cu <sup>2+</sup> )	10	145	55	12	[82]
PPA	3.5	90.9	20	–	[83]
RMC	12	66.7	50	30	[84]
CNT/NFC	7.8	60.7	200	250	[86]
CNT/PMIA	20	230	15	15	[88]
CCNT/PMIA	25	242	12	–	[89]
HCCAFs	2.5	179.6	20	30	[90]
CNT@MXene/CF	4	156	–	–	[91]
MCPs	15	210	30	30	[96]
M-fabric	6	100	20	50	[97]
MS fabric	9	90	30	55	[98]
MXene/BF	3	65.3	180	–	[100]
CNF/MXene-TA	12.5	90	40	40	[101]
CMP	9	100.14	12	6	[102]
BC/PM	6	85	20	40	[103]
ANF/MXene	4	150	15	8	[104]
CCA	3.7	48	30	–	[107]
Ag/AFP	2	126	5.5	5	[108]
AFP/AgNPs	1	210	25	20	[109]
cotton/TA/AgNPs/PDMS	2	118	150	15	[110]
ANF/AgNWs	2.5	200	13	–	[111]
NFC/AgNWs	2	220	–	–	[112]
cellulose/AgNWs	2	99.5	20	–	[113]
silk microfibrils/Ag	7	160	30	–	[114]
Co@ NCNT/CF	2.5	160.2	10	10	[115]
MAg/CNF	2.5	86	70	25	[116]
LCHM	10	120	–	–	[117]
MXene/cellulose/ZnO	3	130	40	–	[118]
LZCFM	2	77.5	45	–	[119]
Cotton/PEDOT: PSS	40	95	95	70	[120]
CMPC	3	30	–	–	[121]
CMP	6	140	30	25	[122]

thermal performance when electromagnetic waves and charges enter parallel to the wood. When a voltage of 2.5 V is applied to C-Wood along the growth direction, its heating temperature can reach up to 100 °C. Thanks to these excellent properties, this easily prepared carbonized wood has great application prospects in the fields of intelligent electronics and electric heating instruments. Dai et al. [125] also obtained carbonized wood with good Joule thermal properties through a similar method. It has a heating temperature of 28.0–83.5 °C under an applied voltage of 0.5–2.0 V (Fig. 15(B)). Carbon Aerogel has the advantages of low density, high specific surface area, and good conductivity. Cellulose-based carbon Aerogel materials have been used in the field of microwave absorbing and electric heating dual functional materials. As shown in Fig. 15(C), Liu et al. [126] prepared 3D carbon Aerogel with nano spiral structure by impregnating and carbonizing bacterial cellulose (BC). Due to the high conductivity between carbonized BC and metal, the Aerogel shows an ultra-high electric heating temperature of 225 °C at a low voltage of 4 V.

In addition, there are some meaningful research works on 3D cellulose-based Joule thermal materials in the fields of crude oil separation and water evaporation. For example, Wu et al. [4] modified a carbonized wood carbon sponge with PDMS(PDMS@WCS) to obtain a compressible cellulose-based composite material for separating crude oil. Under the action of Joule heating, the separation speed of PDMS@WCS for crude oil has been significantly improved. The composite material can generate Joule heat at 75 °C under an applied voltage of 4 V. Fig. 15(D) shows the crude oil separation process. In the absence of external voltage, there is no change in the crude oil after 120 s. After applying the voltage, the crude oil can penetrate within 45 s PDMS@WCS inside the sponge. This is mainly due to the external voltage, PDMS@WCS heat generated greatly reduces the viscosity of crude oil. And thanks to

the abundant pore structure inside the wood, it provides sufficient pathways for the flow of crude oil. In addition, the photothermal effect can accelerate PDMS@WCS The separation effect on crude oil. Benefiting from the uniformly distributed pore structure, the wood-based electric heating device also has certain applications in the field of Water purification. Wang's group [128] directly carbonized wood to obtain a natural wood conductive foam (ACCF) water evaporator for electrothermal/photothermal enhancement. The carbonized wood has excellent electrical conductivity, reaching a high temperature of 145.2 °C at an applied voltage of only 2 V. Thanks to the excellent electrothermal response of ACCF, the evaporation rate of the composite material was increased from 2.25 kg m<sup>-2</sup> h<sup>-1</sup> to an astonishing 6.73 kg m<sup>-2</sup> h<sup>-1</sup> under solar irradiation using a voltage of 2 V for electrothermal compensation. Due to the large pore size of the wood surface, it is difficult to achieve hydrophobic effects, which is not conducive to the continuous improvement of evaporator performance. Based on this, introducing a hydrophobic layer on its surface to enhance the evaporation rate is a good optimization method. As shown in Fig. 15(E), Wu et al. [129] generated a large number of grooves on the surface of wood by KOH activation and then coated them with polyvinyl alcohol (PVA). Finally, the coated PVA layer is exposed to the candle flame to form a hydrophobic layer of carbon nanoparticles, resulting in a CSP-GACW composite material. The prepared composite material has photothermal and electrothermal conversion capabilities, and both of these properties can accelerate the rate of water evaporation by CSP-GACW. In the absence of solar irradiation, when the applied voltage is 6 V, the composite material exhibits a water evaporation rate of 6.86 kg m<sup>-2</sup> h<sup>-1</sup>. Under sunny conditions, CSP-GACW has a water evaporation rate of 11.73 kg m<sup>-2</sup> h<sup>-1</sup> thanks to the synergistic effect of light and heat and electric heating.



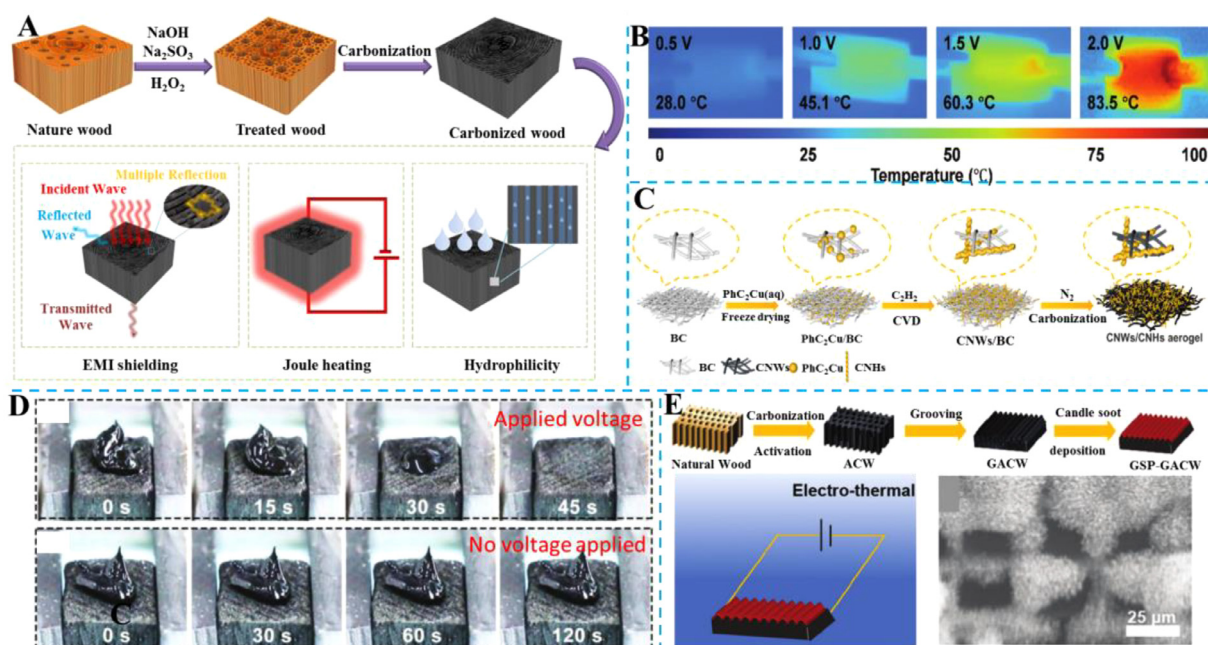


**Fig. 15.** (A) Schematic diagram of the preparation process and application of C-Wood [124]. (B) Infrared temperature images of carbonized wood at different voltages [125]. (C) The preparation process of 3D carbon Aerogel [126]. (D) PDMS@WCS crude oil separation process assisted by Joule heat [127]. (E) The preparation process of CSP-GACW composite materials [128].

### 2.3.2. 3D cellulose/carbon composite materials

Among carbon materials, graphene and carbon nanotubes have the necessary conditions to form an aerogel structure. This also makes these two materials the optimal choice for preparing 3D electric heating devices by combining them with cellulose. Moreover, due to its small micro size, conductive wood can be obtained by combining it with wood through vacuum impregnation. Zhou et al. [130] freeze-dried nanofibrillar cellulose (NFC), multi-wall carbon nanotubes (MWCNTs), and graphene (GP) to prepare 3D Aerogel materials (NFC/MWCNTs/GP) for electric heating. When the concentration of the electroactive substance reaches 5 mg mL<sup>-1</sup>, the conductive gel shows heating performance at 62.0 °C. It is obvious that the mechanical properties of 3D cellulose conductive gel materials prepared by simple blending cannot meet the requirements of electric heating devices for human movement. In order to obtain 3D cellulose Aerogel electric heating materials with higher mechanical strength, the mechanical properties of Aerogel can be effectively improved by using cellulose fabrics and polymers (such as polyethylene glycol) as reinforcement matrix or reinforcement. In addition, the insulation effect is also an important application performance of electric heating devices. As shown in Fig. 16(A), Guo et al. [131] constructed a laminated conductive fabric composed of CNT/cellulose Aerogel, cellulose cotton fabric, and copper nanowires (CuNWs). In this structure, the 3D Aerogel structure provides excellent thermal insulation performance for conductive fabrics and has good photothermal conversion capability. The conductive layer constructed by CuNWs is directly used for the electric heating layer in contact with the human body. Thanks to the high conductivity of CuNWs, conductive fabrics exhibit Joule thermal properties of 40–70.2 °C at a lower voltage of 1–1.8 V (Fig. 16(B)).

In order to obtain 3D cellulose-based Aerogel electric heating composites with higher strength and compression performance, Liu et al. [132] obtained 3D Aerogel electric heating devices with excellent mechanical properties by surface modification of cellulose and impregnation of polyethylene glycol. Fig. 16(C) shows the preparation process of the composite material. First, CNFs were extracted from Sargassum and then surface modified with *tert* butyl

acetoacetic acid. Then CNF/CNT Aerogel was prepared by freeze drying. Finally, CNF/CNT/PEG composite materials were obtained by vacuum impregnation with polyethylene glycol (PEG). The results show that the CNF/CNT Aerogel with crosslinked structure has a compressive strength of 22.6 KPa. This result is obviously better than that of CNF/CNT Aerogel without surface treatment. Under an applied voltage of 6 V, the composite material exhibits a Joule thermal performance of 89.3 °C. It is worth mentioning that the high-temperature melting of PEG endows the composite material with excellent electric energy storage efficiency (85.6 %). Fig. 16(D) shows the temperature-time relationship curve of CNF/CNT/PEG under 6 V voltage. After applying voltage, the temperature of the composite material rapidly rises to the melting point of PEG (51.6 °C). The melting process of PEG absorbing heat creates the first temperature plateau (storage heat) in the temperature time curve. Then, under the action of an applied voltage, the temperature of the composite material continues to rise. Finally, after the voltage is disconnected, the temperature of the heating device rapidly decreases until a second temperature plateau appears (releasing heat). This is due to the crystallization of PEG causing its internal heat dissipation. After PEG is fully crystallized, the temperature of the device rapidly drops to room temperature to complete the heat storage release process. This work utilizes the physical properties of polymer materials to achieve a controllable process of heat storage and release. This provides a new approach for the development of electric heating devices. In order to achieve better electrical heating performance, combining metal materials with carbon materials can effectively improve their conductivity and Joule thermal performance. As shown in Fig. 16(E), Yan et al. [133] obtained ANFs/CNTs/MXene composite Aerogel by freeze-drying. The surface temperature of Aerogel reached 104 °C at 8 V under the synergistic conductive network of CNTs and MXene. And its electric heating response rate is very fast, which can reach saturation temperature within 3 s after applying voltage.

Compared with carbonized wood, 3D wood cellulose-based electric heating devices prepared by the non-carbonization method have more excellent compression performance and stability. For

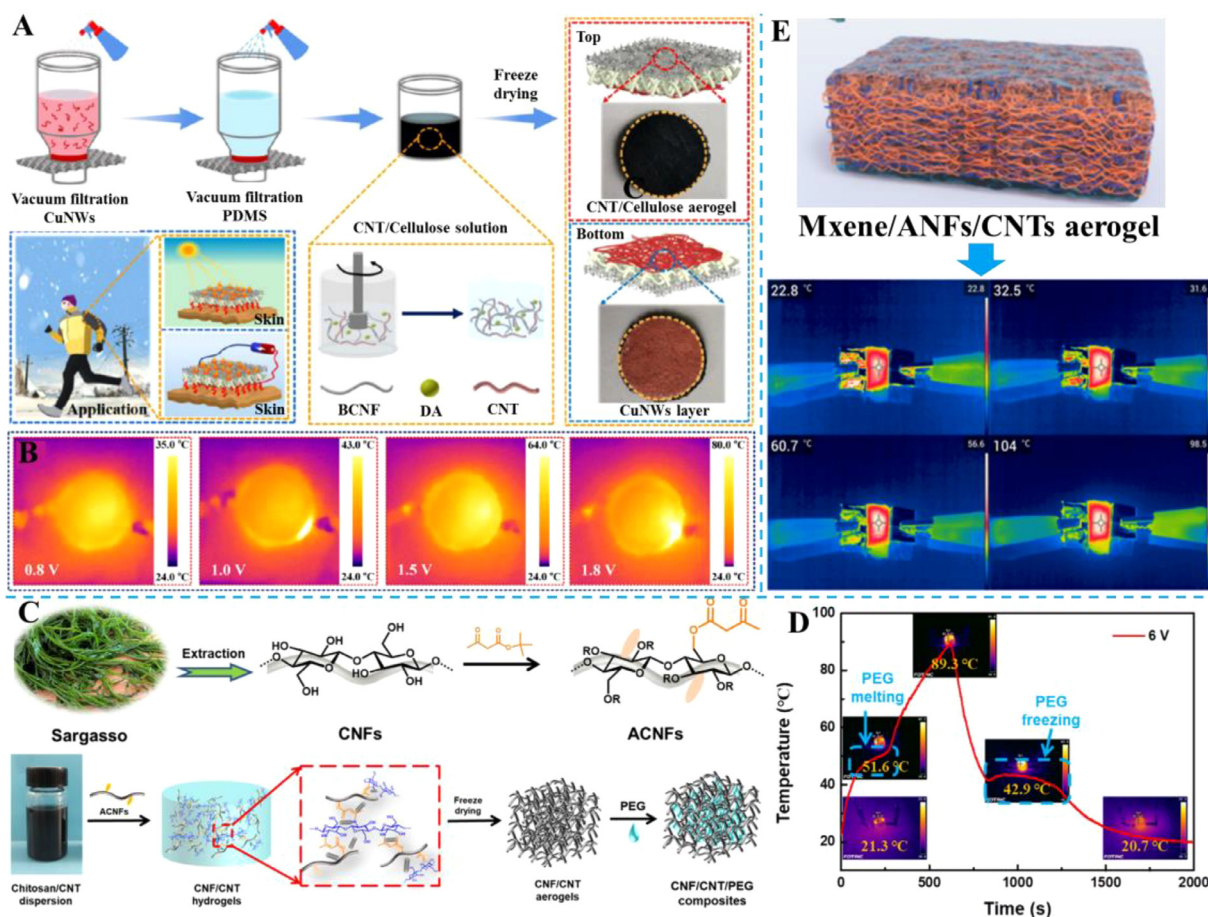


**Fig. 16.** (A) Preparation process and structural schematic diagram of laminated conductive fabric. (B) Infrared temperature images of laminated conductive fabrics at different voltages [131]. (C) The preparation process of CNF/CNT/PEG. (D) Temperature time curve of CNF/CNT/PEG at 6 V [132]. (E) Infrared temperature image of ANFs/CNTs/MXene composite aerogel [133].

example, Chen et al. [134] reported a non-carbonized wood-based crude oil/water separation composite material reinforced by electric heating. Firstly, the material is treated with lignin removal to obtain wood with a more uniform pore structure. Then, the delignified wood is placed in the reduced graphite oxide dispersion, and the conductive wood is obtained after 6 times vacuum impregnation. Finally, superhydrophobic wood with excellent Joule heat and photothermal properties was obtained by coating PDMS on its surface. Through the synergistic effect of Joule heat and photothermal, the surface temperature of the material can reach 139 °C, and the crude oil/water separation rate can reach up to  $1.78 \times 10^5 \text{ kg m}^{-3}$ . Therefore, the superhydrophobic conductive wood obtained from this work has great potential for application in the field of crude oil purification. And this work provides a reference for the preparation of 3D wood cellulose-based electric heating functional devices using non-carbonization methods.

### 2.3.3. 3D cellulose/metal composite materials

Cellulose materials, including bacterial cellulose, nanocellulose, and wood cellulose for lignin removal, provide sufficient skeletal structures for metal materials. The preparation of 3D cellulose/metal Joule thermal composites can be achieved through in-situ growth, blending, and freeze-drying methods. Ma et al. [135] reported that a porous and compressible cellulose-based Aerogel material was obtained by in-situ growth and carbonization with BC as the skeleton structure. Fig. 17(A) shows the preparation process of Aerogel. Firstly, bimetallic CoZn-MOF was in situ grown

in BC Aerogel. Then carbonize it in inert gas to obtain carbon Aerogel material. After carbonization and metal loading, the Aerogel shows  $1.3 \text{ S m}^{-1}$  conductivity. It has a heating performance of 23.3–65.3 °C in the voltage range of 1–9 V. As a two-dimensional metal material, MXene can be loaded in cellulose-based Aerogel with a high specific surface area through the impregnation process. As shown in Fig. 17(B), Zhai et al. [136] obtained waste cotton nanofiber cellulose Aerogel (WCF) by treating and processing waste cotton fabrics. Then MXene is deposited inside the cellulose Aerogel by dip coating. In this work, the conductive gel with different conductive properties was obtained by controlling the number of impregnations of MXene. The results show that the WCF/MXene conductive gel has the best electromagnetic shielding (48.1 dB) and electric heating performance when the immersion times reach 12. The heating temperature of conductive cellulose Aerogel is up to 199 °C when the voltage of 3 V is applied. Although the Aerogel showed excellent Joule thermal properties, repeated impregnation greatly wasted the preparation cost and time. Based on this, Xin et al. [137] simply freeze-dried nanocellulose (CNF) and MXene to obtain CNF/MXene Aerogel with good electrical conductivity. In order to increase the waterproof performance for smart clothing, s-CNF/MXene Aerogel is obtained by coating a layer of silicon hydrophobic layer on the surface of Aerogel through the coating process (Fig. 17(C)). Under the action of the hydrophobic layer, s-CNF/MXene Aerogel still has stable Joule thermal performance in humid environments. In the application of electrically heated composite materials, the storage and release of thermal en-



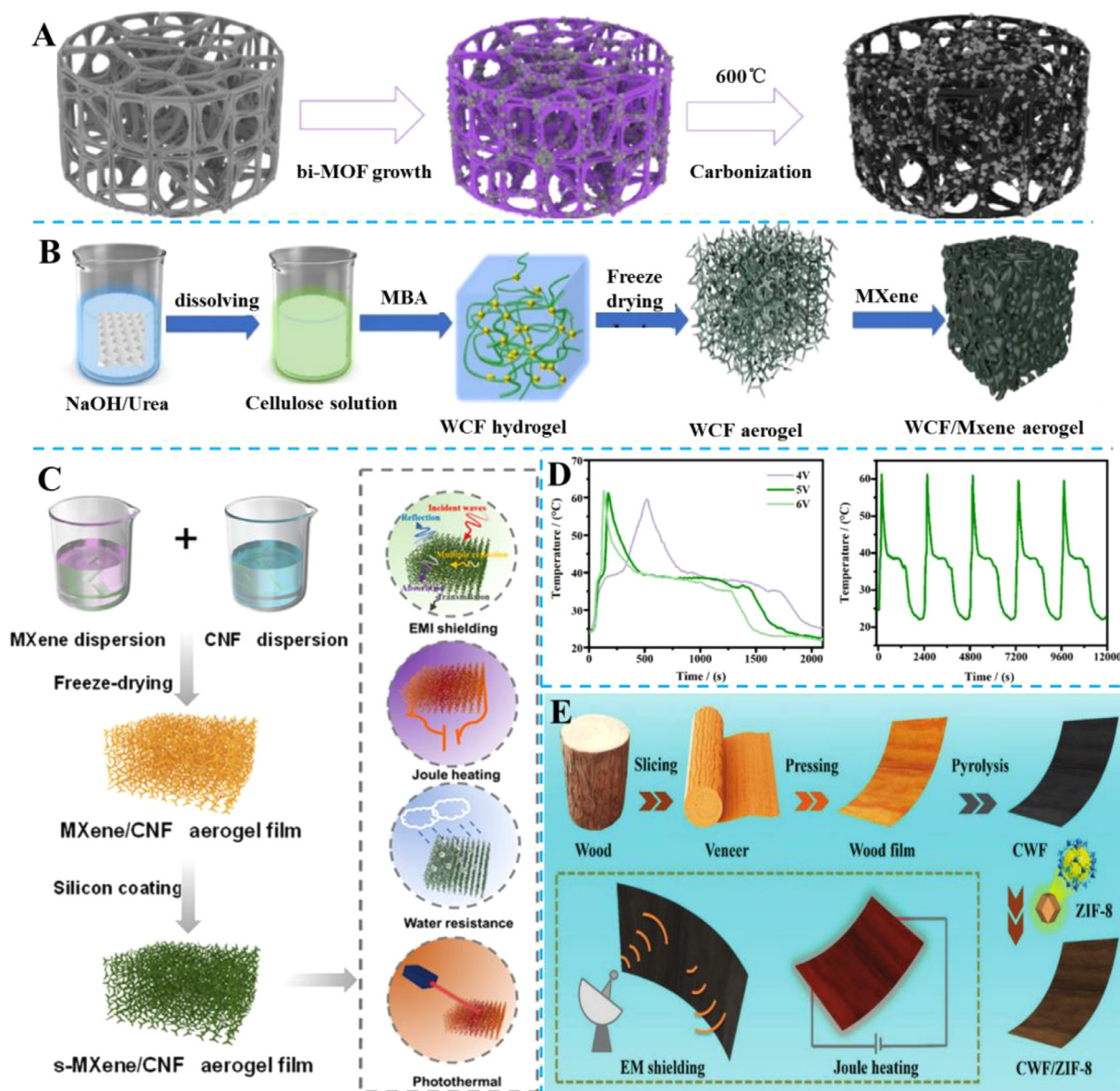


**Fig. 17.** (A) Schematic diagram of the preparation process of BC/CoZn-MOF carbon Aerogel [135]. (B) Preparation process of WCF/MXene Aerogel [136]. (C) S-CNF/MXene Aerogel preparation process and its application diagram [137]. (D) The temperature-time curve of PMCKA composite material under applied voltage [138]. (E) Schematic diagram of CWF/ZIF-8 preparation [139].

ergy are also very important. In addition to the PEG mentioned earlier, it can be used for the storage and release of thermal energy. Huang et al. [138] uniformly blended cellulose nanocrystals (CNCs), MXene, konjac glucomannan, and silver nitrate. The porous light carbon Aerogel was obtained by freeze-drying and annealing. Finally, carbon Aerogel was placed in molten paraffin to obtain PMCKA composite Aerogel with thermal storage performance. Thanks to the phase transition effect of paraffin, PMCKA exhibits excellent thermal storage performance under the action of applied voltage (Fig. 17(D)). In recent research, highly conductive metal materials have also been used to improve the performance of wood-based electric heating devices. As shown in Fig. 17(E), Ma et al. [5,139] prepared ultra-thin wood through carbonization and compression. Then, by in-situ growth of the loaded metal ZIF-8, its conductivity, electromagnetic shielding performance, and Joule thermal performance were improved. The test results show that the surface temperature of the CWF/ZIF-8 electric heater reaches 100 °C at a voltage of 5 V.

### 2.3.4. 3D cellulose/conductive polymer composite materials

Cellulose Aerogel has the advantages of being lightweight, high specific surface area, adjustable porous structure, and low cost [140]. Its porous structure is very conducive to the construction of continuous high-conductivity networks through in-situ polymerization of conductive polymers. Su et al. [141] reported a composite Aerogel with excellent mechanical properties, waterproof properties, and air permeability. Fig. 18(A) shows the preparation process of composite Aerogel. Firstly, CNF Aerogel with a porous structure was obtained by freeze-drying. Then a continuous PPy conductive network is formed in the CNF Aerogel by in-situ polymerization. Finally, CNF/PPy/PU (CPP) aerogel was synthesized by compounding with elastic polyurethane (PU). As shown in Fig. 18(B), PPy forms a continuous conductive network on the cell wall surface of CNF Aerogel. In Aerogel, PU avoids the PPy conductive network falling off during use and prolongs the service life of the device. In electric heating applications, CPP Aerogel has an ultra-high heating temperature of 173 °C at 4 V. And CPP can maintain good elec-

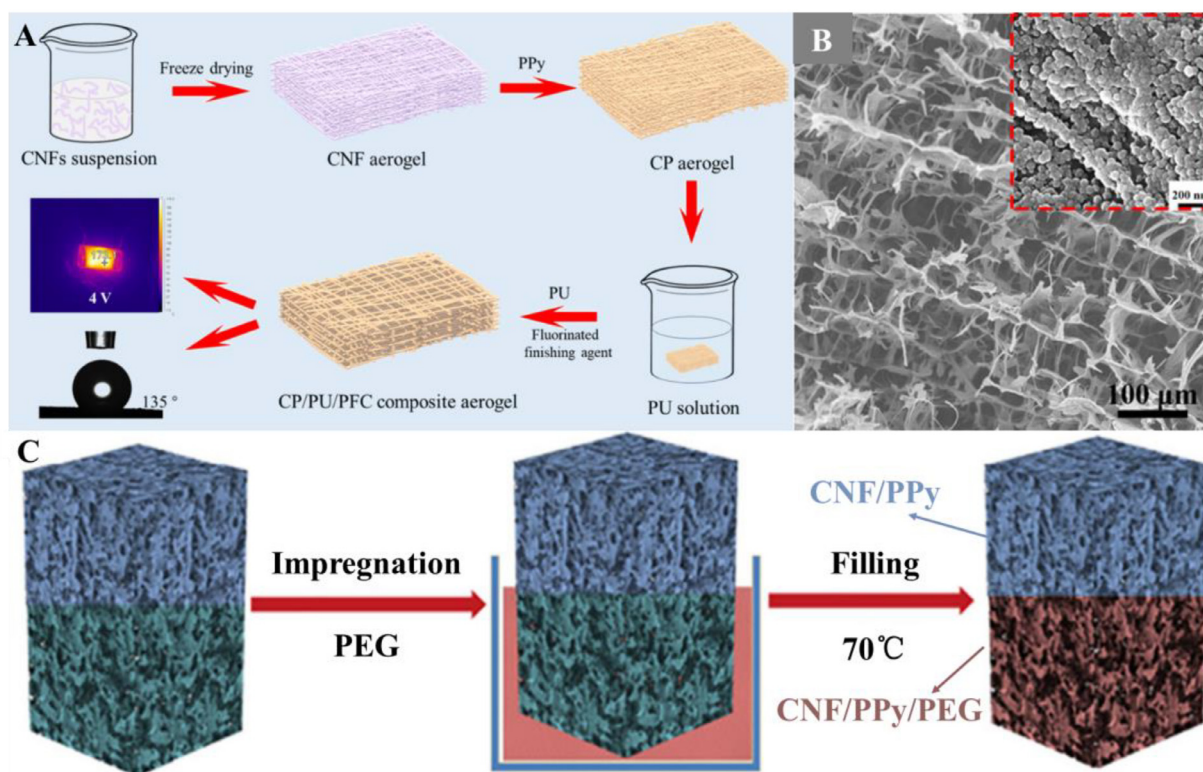


**Fig. 18.** (A) The preparation process of CNF/PU/PPy Aerogel. (B) SEM images of CNF/PU/PPy Aerogel [141]. (C) The preparation process of asymmetric structure electric heating devices [142].

trical heating performance in both stretching and bending states. Similar to the work, Chen et al. [142] prepared 3D-CNf/PPy/PEG Aerogel with thermal storage properties by introducing polyethylene glycol (PEG) on the basis of the previous work (Fig. 18(C)). In this work, the author obtained Aerogel material with thermal insulation by controlling the impregnation area of PEG. In the composite, the Aerogel without PEG impregnation can realize the storage and release of heat energy. The area impregnated with PEG serves as the protection area of heat energy, further reducing the loss of electric heating energy of CNf/PPy Aerogel. In a word, this work uses the phase change properties of PEG and the porous structure of Aerogel to obtain an electric heater that can continuously dissipate heat. And the constructed asymmetric structure has great reference value for the further development of 3D cellulose-based Joule thermal devices. The 3D cellulose-based composite material used for Joule heating devices has excellent pore structure, excellent compression elasticity, and a large heating area. The unique structure mentioned above has enabled its successful application in the fields of crude oil separation, seawater desalination, multifunctional thermal management devices, and electric heating thermal storage materials. Table 3 summarizes the main performance parameters of 3D cellulose Joule thermal composite materials.

### 3. Conclusions and perspectives

With the continuous improvement of people's living standards, various Joule heating devices have attracted widespread attention. Joule thermal devices have shown enormous application value in fields such as personal thermal management, medical equipment, sensing, intelligent devices, and oil/water separation. Among them, cellulose-based Joule thermal devices have excellent mechanical properties and high electrothermal conversion performance, causing a rapidly growing research wave in the field of flexible wear-

ables. So far, cellulose-based Joule thermal devices have been designed in different shapes to meet the application needs of people in different environments. Typically, cellulose-based Joule thermal devices based on 1D include carbonized fibers, conductive yarns, and conductive fibers. Cellulose-based Joule thermal devices based on 2D are typically characterized by conductive fabrics and conductive paper. In addition, 3D structured cellulose-based Joule thermal devices have also been applied in various scenarios in many forms. For example, cellulose-based conductive gel and conductive wood. This article focuses on the design, preparation, and functional application research of cellulose-based Joule thermal composites with different structures such as 1D, 2D, and 3D. And classify and compare them in detail from different materials. Based on the overall content summarized in this article, cellulose-based Joule thermal devices with different structures have their own unique application advantages and microstructure. Table 4 shows the characteristics and applications of 1D, 2D, and 3D cellulose-based Joule thermal composites. It can be seen that cellulose-based Joule thermal composite materials have enormous potential for application in the field of intelligent electronics in the future.

Although significant research progress has been made in cellulose-based Joule thermal devices, there is still great room for development and enormous challenges in their future research and development. In order to promote the further development of cellulose-based Joule heating devices, some key challenges and potential strategies are discussed from the perspective of device development and practical applications (Fig. 19). (1) From the perspective of material preparation, in the preparation process of cellulose-based Joule thermal devices, most of the preparation processes generate significant waste liquid. This is very unfriendly to the environment. For example, during the loading process of conductive substances through in-situ growth, it is inevitable to produce waste liquid containing harmful substances. In future research, we should focus more on researching and de-



**Table 3**  
Performance parameters of 3D cellulose Joule thermal composite materials.

Material	Voltage (V)	Temperature (°C)	Response time (s)	Recovery time (s)	Refs.
C-Wood	2.5	100	90	–	[124]
CW	2.0	83.5	22	50	[125]
CNWs/CNHs	4	225	200	240	[126]
PDMS@WCS	4	75	180	–	[127]
ACCF	2	145.2	180	300	[128]
CSP-GACW	6	63.9	–	–	[129]
NFC/MWCNTs/GP	–	62	500	250	[130]
CNT/ cellulose /CuNWs aerogel	1.8	70.2	80	–	[131]
CNF/CNT/PEG	6	89.3	600	1100	[132]
ANFs/CNTs/MXene	8	104	3	–	[133]
PDMS@GSH wood	20	139	120	80	[134]
bi-MOF@BC	9	65.3	–	–	[135]
WCF/MXene	3	199	–	–	[136]
s-CNF/MXene	10	100	4	1	[137]
PMCKA	6	69	290	810	[138]
CWF/ZIF-8	5	100	10	5	[139]
CPP	4	173	75	175	[141]
3DCNF/PPy/PEG	3	70	120	680	[142]

**Table 4**  
Characteristics and applications of cellulose-based Joule thermal composite materials.

Forms	Feature	Application
1D	Fibre <ul style="list-style-type: none"> <li>◇ Mature continuous production technology</li> <li>◇ Higher aspect ratio</li> </ul>	◇ Multifunctional conductive fibers
	Spinning thread <ul style="list-style-type: none"> <li>◇ Excellent weaving performance</li> </ul>	◇ Thermal management fiber devices based on specific shapes
2D	Film <ul style="list-style-type: none"> <li>◇ Excellent film-forming properties</li> <li>◇ Sufficient mechanical strength</li> <li>◇ Good structural strength</li> </ul>	◇ Electric heating-based actuator
	Paper <ul style="list-style-type: none"> <li>◇ Excellent recyclability</li> <li>◇ Large-scale preparation of paper-based materials</li> <li>◇ Porous structure</li> </ul>	◇ Intelligent. Hyperthermia
	Textile <ul style="list-style-type: none"> <li>◇ Excellent thermal camouflage</li> <li>◇ Multifunctional conductive composite materials</li> </ul>	
	Textile <ul style="list-style-type: none"> <li>◇ High porosity</li> <li>◇ High breathability</li> <li>◇ Comfort based on wearable devices</li> <li>◇ Excellent wear resistance</li> </ul>	◇ Personal thermal management device based on intelligent fabric
	Textile <ul style="list-style-type: none"> <li>◇ Medical field: dilating blood vessels, promoting blood circulation, and drug release based on electric heating</li> </ul>	
3D	Aerogel <ul style="list-style-type: none"> <li>◇ Good compression and rebound performance</li> <li>◇ Lightweight and low-density</li> <li>◇ Excellent thermal insulation performance</li> </ul>	◇ Phase change materials for thermal energy storage
	Aerogel <ul style="list-style-type: none"> <li>◇ Personal thermal management</li> <li>◇ Thermal storage devices</li> </ul>	
	Wood <ul style="list-style-type: none"> <li>◇ Desalination of seawater</li> <li>◇ Crude oil separation</li> <li>◇ Indoor thermal management devices</li> </ul>	

veloping preparation processes that conform to the current global concept of sustainable development with minimal or even no pollution. To further achieve pollution-free preparation and practical application of cellulose-based Joule heating devices. (2) The synchronous improvement of mechanical performance and electric heating performance is also crucial for the development and application of cellulose-based Joule heating devices. In most cellulose-based Joule thermal composites with 1D, 2D, and 3D structures that require blending preparation, the ratio of cellulose to conductive substances plays a decisive role in the performance parameters of the composite material. How to maintain a balance between mechanical performance and electrical heating performance is still a question worth considering. (3) Testing and measurement standards. There is currently no good testing standard or measurement standard for performance parameter testing in all reported work on cellulose-based Joule heat devices. Therefore, it is necessary to develop corresponding testing and performance parameters for cellulose-based Joule thermal devices. This is unfavorable for the practical large-scale application of Joule heating devices, including cellulose-based devices. For example, parameter standards for electric heating devices in application scenarios such as human ther-

mal management, medical rehabilitation, water evaporation, and crude oil separation. (4) Intelligent development and application. Cellulose-based Joule thermal devices exhibit excellent flexibility and mechanical properties. This inevitably leads to adverse factors such as irreversible bending and damage that seriously affect the performance of the device during its use. In future research, it is necessary to develop packaging materials with shape memory performance to ensure the structural stability of devices. Even developing electrically heated composite materials with shape memory function is a method to ensure their structural stability. In addition, the development of self-healing performance of cellulose-based Joule thermal devices can also extend the service life of the devices and greatly reduce maintenance costs. (5) Improvement of accuracy and stability. Improve the correspondence between voltage and temperature during the use of cellulose-based Joule thermal devices. Improving its service life and stability is very important. (6) The large-scale preparation is the main problem that restricts the development of cellulose-based Joule thermal devices. In most of the work currently reported, many are based within the laboratory and have not undergone large-scale preparation testing. However, in the field of cellulose, the combination

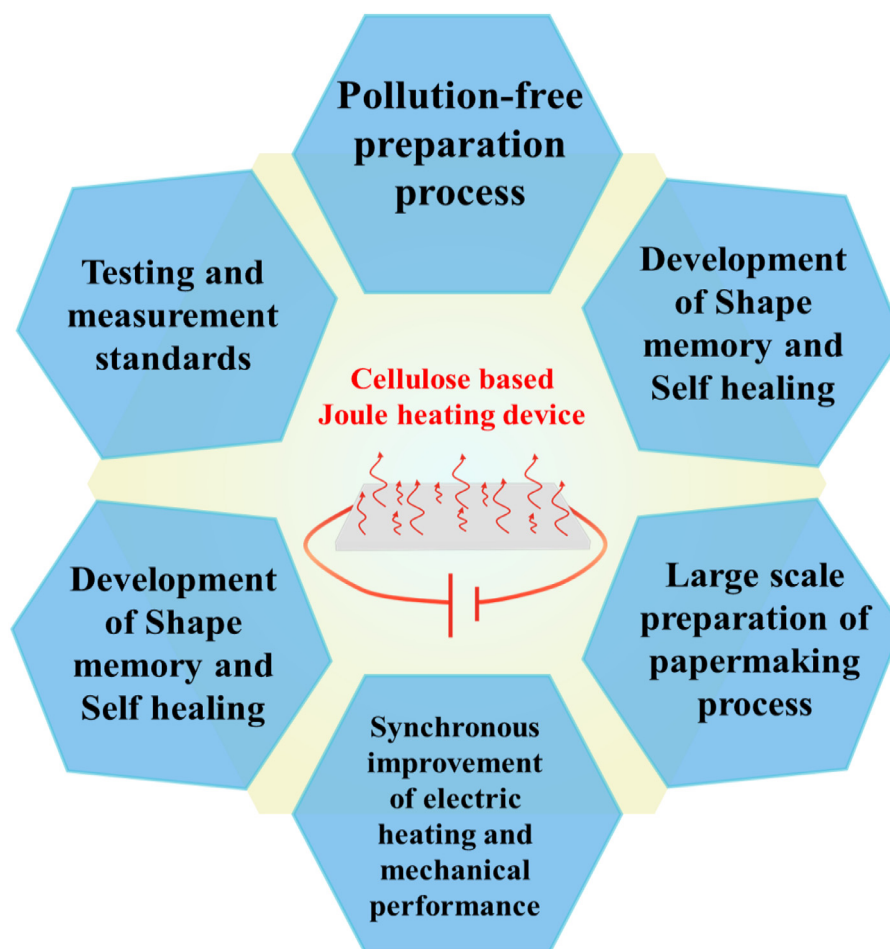


Fig. 19. Future issues and challenges faced by cellulose-based Joule heating devices.

of the papermaking process and controllable spraying process is the most effective way to achieve large-scale preparation of Joule thermal materials. In addition, printing technology can also achieve large-scale preparation of paper-based functional materials. (7) Finally, in the context of green and energy-saving social development, “low voltage-high heat” is an inevitable trend for cellulose-based Joule heat devices. And the development of environmentally friendly and degradable devices is also a future trend. Further efforts are needed to explore the preparation and application of low-cost, high-energy efficient cellulose-based Joule thermal composites. In this article, we summarize the overall research progress of cellulose-based Joule thermal devices. On this basis, the problems and challenges faced in constructing future cellulose-based Joule thermal devices were proposed. At the same time, we hope that some of the insights in this article can provide some reference for future scientific research and promote the efficient preparation of cellulose-based electric heating devices with better performance.

#### Declaration of competing interest

We declare that we have no financial and personal relationships with other people or organizations that can inappropriately influence our work, there is no professional or other personal interest of any nature or kind in any product, service and/or company that could be construed as influencing the position presented in, or the review of, the manuscript entitled, “Recent Advances in Multidimensional (1D, 2D, and 3D) Joule Heating Devices Based on Cellulose: Design, Structure, Application, and Perspective”.

#### Acknowledgments

This work was supported by the fund of the [National Natural Science Foundation of China](#) (Nos. 22378249, 22078184, and 22171170), the [China Postdoctoral Science Foundation](#) (No. 2019M653853XB), and the Natural Science Advance Research Foundation of Shaanxi University of Science and Technology (No. 2018QNBj-03).

#### References

- [1] H.B. Lee, G.K. Veerasubramani, K.S. Lee, H.Y.H. Lee, T.H. Han, *Carbon* 198 (2022) 252–263.
- [2] K.P. Ruan, X.T. Shi, Y.L. Zhang, Y.Q. Guo, X. Zhong, J.W. Gu, *Angew Chem. Int. Edit.* 62 (2023) e202309010.
- [3] D. Zhang, S.W. Xu, X. Zhao, W.Q. Qian, C.R. Bowen, Y. Yang, *Adv. Funct. Mater.* 30 (2020) 1910809.
- [4] L.S. Wu, L. Wang, Z. Guo, J.C. Luo, H.G. Xue, J.F. Gao, *ACS Appl. Mater. Interfaces* 11 (2019) 34338–34347.
- [5] X. Fang, H. Sun, C. Wu, Z. Fang, M. Li, L. Zhao, B. Tian, P. Verma, J. Wang, R. Maeda, Z. Jiang, *ACS Appl. Mater. Interfaces* 15 (2023) 28465–28475.
- [6] S. Gong, X.X. Sheng, X.L. Li, M.J. Sheng, H. Wu, X. Lu, J.P. Qu, *Adv. Funct. Mater.* 32 (2022) 2200570.
- [7] Q.H. Yu, J.J. Pan, J.N. Li, C.A.L. Su, Y.L. Huang, S.Y. Bi, J.H. Jiang, N.L. Chen, *J. Mater. Chem. C* 10 (2022) 13143–13156.
- [8] M.K. Roul, B. Obasogie, G. Kogo, J.R. Skuza, R.M. Mundle, A.K. Pradhan, *J. Appl. Phys.* 122 (2017) 135110.
- [9] M. Ameen, Z. Zhang, X.C. Wang, M. Yaseen, M. Umair, R.S. Noor, W. Lu, K. Yousaf, F. Ullah, M.S. Memon, *Energies* 12 (2019) 933.
- [10] W.T. Hao, J. Xu, R. Li, X.Z. Zhao, L.Z. Qiu, W. Yang, *Chem. Eng. J.* 368 (2019) 837–846.
- [11] C. Chen, Z.C. Huan, Y.L. Jiao, L.A. Shi, Y.Y. Zhang, J.W. Li, C.Z. Li, X.D. Lv, S.Z. Wu, Y.L. Hu, W.L. Zhu, D. Wu, J.R. Chu, L. Jiang, *ACS Nano* 13 (2019) 5742–5752.



- [12] V.B. Nam, J. Shin, Y. Yoon, T.T. Giang, J. Kwon, Y.D. Suh, J. Yeo, S. Hong, S.H. Ko, D. Lee, *Adv. Funct. Mater.* 29 (2019) 1806895.
- [13] M. Saito, E. Kanai, H. Fujita, T. Aso, N. Matsutani, T. Fujie, *Adv. Funct. Mater.* 31 (2021) 2102444.
- [14] Y. Yang, S. Chen, W.L. Li, P. Li, J.G. Ma, B.S. Li, X.N. Zhao, Z.S. Ju, H.C. Chang, L. Xiao, H.Y. Xu, Y.C. Liu, *ACS Nano* 14 (2020) 8754–8765.
- [15] Q. Liu, B. Tian, J. Liang, W. Wu, *Mater. Horizons* 8 (2021) 1634–1656.
- [16] Y. Lee, V.T. Le, J.G. Kim, H. Kang, E.S. Kim, S.E. Ahn, D. Suh, *Versatile, Adv. Funct. Mater.* 28 (2018) 1706007.
- [17] U. Khan, T.H. Kim, K.H. Lee, J.H. Lee, H.J. Yoon, R. Bhatia, I. Sameera, W. Seung, H. Ryu, C. Falconi, S.W. Kim, *Nano Energy* 17 (2015) 356–365.
- [18] S.D. Kang, G.J. Snyder, *Nat. Mater.* 16 (2017) 252–257.
- [19] G. Yang, R.Q. Xing, Y.F. Li, C.Q. Ma, B.W. Cheng, J. Yan, X.P. Zhuang, *Chem. Eng. J.* 426 (2021) 131931.
- [20] O.Y. Qin, X.L. Wang, L. Liu, *Compos. Sci. Technol.* 217 (2022) 109115.
- [21] Y.G. Jeong, J.E. An, *Compos. Pt. A-Appl. Sci. Manuf.* 56 (2014) 1–7.
- [22] C.Y. Xiong, Y.K. Zhang, Y.H. Ni, J. Power Sources 560 (2023) 232698.
- [23] Y. Ko, G. Kwon, H. Choi, K. Lee, Y. Jeon, S. Lee, J. Kim, J. You, *Adv. Funct. Mater.* 33 (2023) 2302785.
- [24] K. Bethke, S. Palantoken, V. Andrei, M. Ross, V.S. Raghuvanshi, F. Kettemann, K. Greis, T.T.K. Ingber, J.B. Stuckrath, S. Valiyaveetil, K. Rademann, *Adv. Funct. Mater.* 28 (2018) 1800409.
- [25] C.Y. Xiong, T.X. Wang, Y.K. Zhang, M. Zhu, Y.H. Ni, *Nano Res.* 15 (2022) 7506–7532.
- [26] X. Tao, D.X. Tian, S.Q. Liang, P. Jiang, L.F. Zhang, F. Fu, *ACS Appl. Energy Mater.* 5 (2022) 13096–13112.
- [27] Z.H. Shen, M.L. Qin, F. Xiong, R.Q. Zou, J. Zhang, *Energy Environ. Sci.* 16 (2023) 830–861.
- [28] C.H. Yang, M. Nie, Y.S. Liu, *Compos. Sci. Technol.* 238 (2023) 110045.
- [29] S. Shin, S. Park, A. Toor, H.Y. So, *Cellulose* 30 (2023) 6119–6147.
- [30] J.S. Lee, H. Jo, H.S. Choe, D.S. Lee, H. Jeong, H.R. Lee, J.H. Kweon, H. Lee, R.S. Myong, Y. Nam, *Compos. Struct.* 289 (2022) 115510.
- [31] S. Sheykhnazari, T. Tabarsa, M. Mashkour, A. Khazaeian, A. Ghanbari, *Int. J. Biol. Macromol.* 120 (2018) 2115–2122.
- [32] H.C. Chang, Y. Jia, L. Xiao, H.H. Chen, K. Zhao, Y.S. Chen, Y.F. Ma, *Carbon* 154 (2019) 150–155.
- [33] J.W. Xie, Y.H. Zhang, J.M. Dai, Z.X. Xie, J. Xue, K. Dai, F. Zhang, D. Liu, J.Y. Cheng, F.Y. Kang, B.B. Li, Y. Zhao, L. Lin, Q.B. Zheng, *Small* 19 (2023) 2205853.
- [34] Y.X. Han, K.P. Ruan, J.W. Gu, *Angew Chem. Int. Edit.* 62 (2023) e202216093.
- [35] K.S. Moreira, D. Lermen, L.P. dos Santos, F. Galembeck, T.A.L. Burgo, *Energy Environ. Sci.* 14 (2021) 353–358.
- [36] S.H. Kim, H.C. Ko, J. Mater. Chem. C 7 (2019) 14525–14534.
- [37] D. Janas, K.K.K. Koziol, *Appl. Surf. Sci.* 376 (2016) 74–78.
- [38] Y. Zhou, X.J. Wang, X.D. Liu, D.K. Sheng, F.C. Ji, L. Dong, S.B. Xu, H.H. Wu, Y.M. Yang, *Carbon* 142 (2019) 558–566.
- [39] S.R. Tan, J.S. Wang, W.H. Jin, Q. Zhang, Z. Zhao, D.Q. Li, D.S. Cheng, S.G. Bi, J.H. Ran, G.M. Cai, X. Wang, *Compos. Commun.* 37 (2023) 101446.
- [40] L.C. Jia, W.J. Sun, L. Xu, J.F. Gao, K. Dai, D.X. Yan, Z.M. Li, *Ind. Eng. Chem. Res.* 59 (2020) 7546–7553.
- [41] J.G. Lee, S. An, T.G. Kim, M.W. Kim, H.S. Jo, M.T. Swihart, A.L. Yarin, S.S. Yoon, *ACS Appl. Mater. Interfaces* 9 (2017) 35325–35332.
- [42] Y.X. Han, K.P. Ruan, J.W. Gu, *Nano Res.* 15 (2022) 4747–4755.
- [43] P. Isacson, K. Jain, A. Fall, V. Chauve, A. Hajian, H. Granberg, L. Boiron, M. Berggren, K. Hakansson, J. Edberg, I. Engquist, L. Wagberg, *J. Mater. Chem. A* 10 (2022) 21579–21589.
- [44] D.D. Li, W.Y. Lai, Y.Z. Zhang, W. Huang, *Adv. Mater.* 30 (2018) 1704738.
- [45] P. Yang, S. Ghosh, T. Xia, J.C. Wang, M.A. Bissett, I.A. Kinloch, S. Barg, *Compos. Sci. Technol.* 218 (2022) 109199.
- [46] R.Q. Ye, Y. Chyan, J.B. Zhang, Y.L. Li, X. Han, C. Kittrell, J.M. Tour, *Adv. Mater.* 29 (2017) 1702211.
- [47] M. Molco, F. Laye, E. Samperio, S.Z. Sharabani, V. Fourman, D. Sherman, M. Tsotsalas, C. Woll, J. Lahann, A. Sitt, *ACS Appl. Mater. Interfaces* 13 (2021) 12491–12500.
- [48] D.C. Wang, H.Y. Yu, D.M. Qi, Y.H. Wu, L.M. Chen, Z.H. Li, *J. Am. Chem. Soc.* 143 (2021) 11620–11630.
- [49] D.Q. Li, J.F. Wang, X. Lu, W. Chen, X.W. Dong, B. Tang, X.G. Wang, *Mater. Des.* 181 (2019) 107941.
- [50] C.Y. Xiong, C.M. Zheng, B.B. Li, Y.H. Ni, *Ind. Crops Prod.* 178 (2022) 114565.
- [51] L.S. Xie, G. Skorupskii, M. Dinca, *Chem. Rev.* 120 (2020) 8536–8580.
- [52] M. Abutalip, G. Zhigerbayeva, D. Kanzhigitova, P. Askar, Y. Yeszhan, T.T. Pham, S. Adilov, R. Luque, N. Nuraje, *Adv. Mater.* 35 (2023) 2208864.
- [53] C.Y. Xiong, B.B. Li, X. Lin, H.G. Liu, Y.J. Xu, J.J. Mao, C. Duan, T.H. Li, Y.H. Ni, *Compos. Pt. B-Eng.* 165 (2019) 10–46.
- [54] M. Ahmad, S.R.P. Silva, *Carbon* 158 (2020) 24–44.
- [55] S. Uzun, S. Seyedin, A.L. Stoltzfus, A.S. Levitt, M. Alhabeb, M. Anayee, C.J. Strobil, J.M. Razal, G. Dion, Y. Gogotsi, *Adv. Funct. Mater.* 29 (2019) 1905015.
- [56] B. Wu, Y. Liu, H. Yu, *J. Appl. Polym. Sci.* 139 (2022) e53014.
- [57] C.F. Jing, W.H. Liu, H.L. Hao, H.G. Wang, F.B. Meng, D. Lau, *Nanoscale* 12 (2020) 16305–16314.
- [58] J.H. Ma, H.H. Pu, P.X. He, Q.L. Zhao, S.X. Pan, Y.W. Wang, C. Wang, *Cellulose* 28 (2021) 7877–7891.
- [59] H.C. Kim, H.A. Sodano, *Adv. Funct. Mater.* 33 (2023) 2208661.
- [60] C.A.C. Chazot, B. Damirchi, B. Lee, A.C.T. van Duin, A.J. Hart, *Nano Lett.* 22 (2022) 998–1006.
- [61] P.X. He, H.H. Pu, X.F. Li, X.Q. Hao, J.H. Ma, *J. Appl. Polym. Sci.* 140 (2023) e53668.
- [62] W.T. Koo, S.J. Kim, J.S. Jang, D.H. Kim, I.D. Kim, *Adv. Sci.* 6 (2019) 1900250.
- [63] G.C. Hu, H. Zhao, N. Zhong, H. Zhao, H.G. Zhang, A.M. Zang, F.G. Kong, J.G. Hu, *ACS Appl. Polym. Mater.* 5 (2023) 3338–3347.
- [64] L. Wang, M.Y. Zhang, B. Yang, J.J. Tan, *ACS Appl. Mater. Interfaces* 13 (2021) 41933–41945.
- [65] S. Haldar, D. Rase, P. Shekhar, C. Jain, C.P. Vinod, E. Zhang, L. Shupletsov, S. Kaskel, R. Vaidhyanathan, *Adv. Energy Mater.* 12 (2022) 2200754.
- [66] S. Lee, C.H. Park, *RSC Adv.* 8 (2018) 31008–31018.
- [67] J.C. Lv, Y.M. Dai, H. Xu, Y. Zhong, L.P. Zhang, Z.Z. Chen, X.F. Sui, X.L. Feng, B.J. Wang, Z.P. Mao, *J. Mater. Chem. C* 8 (2020) 1309–1318.
- [68] K. Pattanarat, N. Petchsang, T. Osotchan, Y.H. Kim, R. Jaisutti, *ACS Appl. Mater. Interfaces* 13 (2021) 48053–48060.
- [69] M.D.V. Tinoco, L.R. Fujii, C.Y.N. Nicoliche, G.F. Giordano, J.A. Barbosa, J.F. da Rocha, G.T. dos Santos, J. Bettini, M. Santhiago, M. Strauss, R.S. Lima, *Nanoscale* 15 (2023) 6201–6214.
- [70] R. Ghosh, S. Telpande, P. Gowda, S.K. Reddy, P. Kumar, A. Misra, *ACS Appl. Mater. Interfaces* 12 (2020) 29959–29970.
- [71] W.G. Kim, D. Kim, H.M. Lee, Y.K. Choi, *Nano Energy* 100 (2022) 107485.
- [72] T. Gabrys, B. Fryczkowska, D. Binias, C. Slusarczyk, J. Fabia, *Carbohydr. Polym.* 254 (2021) 117436.
- [73] S.H. Kim, J.M. Kim, D.B. Ahn, S.Y. Lee, *Small* 16 (2020) 2002837.
- [74] S.M. Goodman, I.A. Tortajada, F. Haslbeck, K.Y. Oyulmaz, A. Rummier, C.S. Sanchez, J.T. Pais, H. Denizli, K.J. Haunreiter, A.B. Dichiaro, *Nano Today* 40 (2021) 101270.
- [75] W. Zhang, X.X. Ji, M.G. Ma, *Chem. Eng. J.* 458 (2023) 141402.
- [76] R. Kumar, A.P. del Pino, S. Sahoo, R.K. Singh, W.K. Tan, K.K. Kar, A. Matsuda, E. Joanni, *Prog. Energy Combust. Sci.* 91 (2022) 100981.
- [77] S. Xia, M. Wang, G.H. Gao, *Nano Res.* 15 (2022) 9850–9865.
- [78] R. Menzel, S. Barg, M. Miranda, D.B. Anthony, S.M. Bawaked, M. Mokhtar, S.A. Al-Thabaiti, S.N. Basahel, E. Saiz, M.S.P. Shaffer, *Adv. Funct. Mater.* 25 (2015) 28–35.
- [79] X.P. Li, C. Shao, B. Zhuo, S. Yang, Z.Y. Zhu, C.W. Su, Q.P. Yuan, *Int. J. Biol. Macromol.* 139 (2019) 1103–1116.
- [80] S. Tanpichai, A. Boonmahitthisud, N. Soykeabkaew, L. Ongthip, *Carbohydr. Polym.* 286 (2022) 119192.
- [81] X.D. Tan, Y.Z. Jiang, Q.Y. Peng, T. Subrova, J. Saskova, J. Wiener, M. Venkataraman, J. Militky, P. Kejzlar, A.R. Mahendran, H. Lammer, W. Xiong, *Cellulose* 30 (2023) 4561–4574.
- [82] Y. Yang, C.L. Luo, X.D. Chen, M. Wang, *Compos. Sci. Technol.* 233 (2023) 109913.
- [83] X. Li, H.F. Yang, S.R. Lu, R. Cai, *Adv. Mater. Technol.* 8 (2023) 2300079.
- [84] X.H. Zheng, W.Q. Nie, Q.L. Hu, X.W. Wang, Z.Q. Wang, L.H. Zou, X.H. Hong, H.W. Yang, J.K. Shen, C.L. Li, *Mater. Des.* 200 (2021) 109442.
- [85] W.J. Sun, C.G. Zhou, L.C. Jia, Y.Y. Wang, Y.P. Zhang, T. Wang, D.X. Yan, Z.M. Li, *J. Mater. Chem. C* 8 (2020) 8814–8822.
- [86] X.P. Li, H.J. Zou, B. Zhuo, C. Shao, S.A. Cao, B.X. Zhang, Q.P. Yuan, *Langmuir* 37 (2021) 5763–5775.
- [87] R. Ghosh, A. Misra, *ACS Appl. Electron. Mater.* 3 (2021) 1260–1267.
- [88] B. Yang, X.Y. Ding, M.Y. Zhang, L. Wang, *Compos. Pt. B-Eng.* 224 (2021) 109242.
- [89] L. Wang, M.Y. Zhang, B. Yang, X.Y. Ding, J.J. Tan, S.X. Song, J.Y. Nie, *ACS Appl. Mater. Interfaces* 13 (2021) 5486–5497.
- [90] Y. Chen, C.Z. Zhang, S.M. Tao, H.T. Chai, D.F. Xu, X.X. Li, H.S. Qi, *Chem. Eng. J.* 466 (2023) 143153.
- [91] Y.H. Zhang, W. Wang, J.W. Xie, K. Dai, F. Zhang, Q.B. Zheng, *Carbon* 200 (2022) 491–499.
- [92] A. Pajor-Swierzy, K. Szczepanowicz, A. Kamysny, S. Magdassi, *Adv. Colloid Interface Sci.* 299 (2022) 102578.
- [93] D. Doganay, M.O. Cicek, M.B. Durukan, B. Altuntas, E. Agbahca, S. Coskun, H.E. Unalan, *Nano Energy* 89 (2021) 106412.
- [94] Y. Liu, Q. Wang, *Nat. Mater.* 22 (2023) 814–815.
- [95] Y.J. Huo, B.C. Wang, A.M. Nie, C.P. Mu, J.Y. Xiang, K. Zhai, T.Y. Xue, F.S. Wen, *ACS Appl. Nano Mater.* 5 (2022) 5589–5598.
- [96] S.Y. Kim, H.E. Gang, G.T. Park, H.B. Jeon, Y.G. Jeong, *Adv. Eng. Mater.* 23 (2021) 2100548.
- [97] X. Zhao, L.Y. Wang, C.Y. Tang, X.J. Zha, Y. Liu, B.H. Su, K. Ke, R.Y. Bao, M.B. Yang, W. Yang, *ACS Nano* 14 (2020) 8793–8805.
- [98] H. Li, Y.N. Pan, Z.Q. Du, *Cellulose* 29 (2022) 8427–8441.
- [99] Y.Q. He, J. Yang, W.T. Chen, W. Chen, L. Zhao, W. Qi, *Chem. Eng. J.* 464 (2023) 142565.
- [100] W.B. Zhu, F.L. Yi, P. Huang, H. Zhang, Z.H. Tang, Y.Q. Fu, Y.Y. Wang, J. Huang, G.H. Dong, Y.Q. Li, S.Y. Fu, *J. Mater. Chem. A* 9 (2021) 26758–26766.
- [101] J. Wei, S. Jia, C.M. Jie, Z.Q. Shao, *ACS Appl. Mater. Interfaces* 13 (2021) 38700–38711.
- [102] G.Q. Zhou, X. Wang, T. Wan, C.Z. Liu, W.M. Chen, S.H. Jiang, J.Q. Han, Y.G. Yan, M.C. Li, C.T. Mei, *Energy Environ. Mater.* 6 (2023) e12454.
- [103] T.Y. Zhang, B.Q. Song, J. Yang, B.B. Yuan, J.H. Ma, *Cellulose* 30 (2023) 4373–4385.
- [104] J. Wang, X.Y. Ma, J.L. Zhou, F.L. Du, C. Teng, *ACS Nano* 16 (2022) 6700–6711.
- [105] W.Q. Liu, Y. Sun, A.N. Cui, Y.F. Xia, Q.Z. Yan, Y.X. Song, L.L. Wang, G.Y. Shan, X. Wang, *Nano Energy* 105 (2023) 107987.
- [106] M. Kwon, H. Kim, A.K. Mohanty, J. Yang, L.H. Piao, S.W. Joo, J.T. Han, J.H. Han, H.J. Paik, *Adv. Mater. Technol.* 6 (2021) 2100177.

- [107] X.J. Yue, M.Y. He, T. Zhang, D.Y. Yang, F.X. Qu, *ACS Appl. Mater. Interfaces* 12 (2020) 12285–12293.
- [108] S.H. Zhu, C.W. Lou, S.H. Zhang, N. Wang, J.W. Li, Y.J. Feng, R.D. He, C.G. Xu, J.H. Lin, *Surf. Interfaces* 29 (2022) 101689.
- [109] Y.F. Zhou, Z.H. Sun, L. Jiang, S.J. Chen, J.W. Ma, F.L. Zhou, *Ind. Eng. Chem. Res.* 59 (2020) 18898–18906.
- [110] Z.P. Guo, Y.L. Wang, J.J. Huang, S.Y. Zhang, R.Q. Zhang, D.Z. Ye, G.M. Cai, H.J. Yang, S.J. Gu, W.L. Xu, *Cellulose* 28 (2021) 7483–7495.
- [111] Z.L. Ma, S.L. Kang, J.Z. Ma, L. Shao, A.J. Wei, C.B. Liang, J.W. Gu, B. Yang, D.D. Dong, L.F. Wei, Z.Y. Ji, *ACS Nano* 13 (2019) 7578–7590.
- [112] R. Cheng, B. Wang, J.S. Zeng, J.P. Li, J. Xu, W.H. Gao, K.F. Chen, *ACS Appl. Mater. Interfaces* 14 (2022) 30144–30159.
- [113] C.B. Liang, K.P. Ruan, Y.L. Zhang, J.W. Gu, *ACS Appl. Mater. Interfaces* 12 (2020) 18023–18031.
- [114] L.L. Lv, X.S. Han, X.C. Wu, C.X. Li, *ACS Sustain. Chem. Eng.* 8 (2020) 248–255.
- [115] X.C. Zhang, M.J. Liu, J. Xu, Q.Y. Ouyang, C.L. Zhu, X.L. Zhang, X.T. Zhang, Y.J. Chen, *Chem. Eng. J.* 433 (2022) 133794.
- [116] C.B. Liang, J. He, Y.L. Zhang, W. Zhang, C.L. Liu, X.T. Ma, Y.Q. Liu, J.W. Gu, *Compos. Sci. Technol.* 224 (2022) 109445.
- [117] B. Gu, X.Y. Huang, F.X. Qiu, D.Y. Yang, T. Zhang, *ACS Sustain. Chem. Eng.* 8 (2020) 15936–15945.
- [118] B.C. Zhao, C.Z. Li, Y.F. Chen, Q. Tian, Y. Yurekli, F.X. Qiu, T. Zhang, *Cellulose* 30 (2023) 5171–5185.
- [119] B.C. Zhao, H.A. Wu, Q. Tian, Y.Q. Li, F.X. Qiu, T. Zhang, *ACS Appl. Mater. Interfaces* 15 (2023) 8751–8760.
- [120] M.A. Jalil, A. Ahmed, M.M. Hossain, B. Adak, M.T. Islam, M. Moniruzzaman, M.S. Parvez, M. Shkir, S. Mukhopadhyay, *ACS Omega* 7 (2022) 12716–12723.
- [121] Y.N. Li, J. Wang, L.L. Huang, L.H. Chen, H.L. Gao, Y.H. Ni, Q.H. Zheng, *ACS Sustain. Chem. Eng.* 10 (2022) 6414–6425.
- [122] E. Li, Y.M. Pan, C.F. Wang, C.T. Liu, C.Y. Shen, C.F. Pan, X.H. Liu, *Chem. Eng. J.* 420 (2021) 129864.
- [123] C.Y. Xiong, M.R. Li, S.X. Nie, W.H. Dang, W. Zhao, L. Dai, Y.H. Ni, J. Power Sources 471 (2020) 228448.
- [124] B. Zhao, P.W. Bai, S. Wang, H.Y. Ji, B.B. Fan, R. Zhang, R.C. Che, *ACS Appl. Mater. Interfaces* 13 (2021) 29101–29112.
- [125] Z.H. Dai, C.S. Hu, Y.Y. Wei, W.W. Zhang, J.T. Xu, X.Y. Lin, *Adv. Electron. Mater.* 9 (2023) 2300162.
- [126] D.S. Liu, P.P. Mou, Q.Y. Wei, Y. Xu, G.P. Wan, G.Z. Wang, *Carbon* 204 (2023) 7–16.
- [127] M.B. Wu, S. Huang, T.Y. Liu, J. Wu, S. Agarwal, A. Greiner, Z.K. Xu, *Adv. Funct. Mater.* 31 (2021) 2006806.
- [128] W. Fan, C.B. Wang, G.F. Li, Y. Wang, W.H. Zhang, G.L. Shi, X.Y. Yan, J. Shi, *Mater. Today Nano* 23 (2023) 100352.
- [129] J. Wu, X.F. Li, T.T. Zhang, X.P. Li, W. Li, Z.Z. Yu, *Mater. Chem. Front.* 6 (2022) 306–315.
- [130] B. Zhuo, S.A. Cao, X.P. Li, J.H. Liang, Z.H. Bei, Y.T. Yang, Q.P. Yuan, *Molecules* 25 (2020) 3836.
- [131] Z.G. Guo, C. Sun, J. Wang, Z.S. Cai, F.Y. Ge, *ACS Appl. Mater. Interfaces* 13 (2021) 8851–8862.
- [132] Y. Liu, H.C. Liu, H.S. Qi, J. Colloid Interface Sci. 629 (2023) 478–486.
- [133] Z. Yan, Y.L. Ding, M.R. Huang, J.F. Li, Q.X. Han, M.Q. Yang, W.M. Li, *ACS Appl. Nano Mater.* 6 (2023) 6141–6150.
- [134] Z.H. Chen, X.J. Su, W.J. Wu, J.L. Zhou, T. Wu, Y.H. Wu, H.L. Xie, K.Q. Li, *Carbon* 201 (2023) 577–586.
- [135] H. Ma, Z.G. Wang, X.F. Zhang, J.F. Yao, *Ceram. Int.* 49 (2023) 20951–20959.
- [136] J.Y. Zhai, C. Cui, A. Li, R.H. Guo, C. Cheng, E.H. Ren, H.Y. Xiao, M. Zhou, J.W. Zhang, *Ceram. Int.* 48 (2022) 13464–13474.
- [137] W. Xin, M.G. Ma, F. Chen, *A.C.S. Appl. Nano Mater.* 4 (2021) 7234–7243.
- [138] D.Y. Huang, Z.B. Wang, X.X. Sheng, Y. Chen, *Sol. Energy Mater. Sol. Cells* 251 (2023) 112124.
- [139] X.F. Ma, J.J. Pan, H.T. Guo, J.W. Wang, C.M. Zhang, J.Q. Han, Z.C. Lou, C.X. Ma, S.H. Jiang, K. Zhang, *Adv. Funct. Mater.* 33 (2023) 2213431.
- [140] M. Wang, X.Z. Zhang, C.L. Chen, Y. Wen, Q.C. Wen, Q. Fu, H. Deng, J. Mater. Chem. A 11 (2023) 7711–7723.
- [141] Y.T. Wang, L.Y. Chen, H. Cheng, B.J. Wang, X.L. Feng, Z.P. Mao, X.F. Sui, *Chem. Eng. J.* 402 (2020) 126222.
- [142] L.Y. Chen, H.N. Zhang, Z.P. Mao, B.J. Wang, X.L. Feng, X.F. Sui, *Carbohydr. Polym.* 288 (2022) 119409.